The position of the surface of a reference specimen is often adjusted using a mechanical micrometer device, in which case a thin metal plate of accurately known thickness can be put between the powder and the device to facilitate accurate positioning of the surface.

11.2.2 Method of measurement

The measurement angles 2θ and ψ used for the reference specimen should be comparable to those used in the subsequent experiments. The measurement time can be increased to reduce counting statistical errors. The acceptance of the obtained values shall be made following the criteria stated in clause 8.4.

11.3 Stress-reference specimen

11.3.1 Laboratory qualified (LQ) stress-reference specimen

If a laboratory creates a reference specimen which contains a known level of stress it is called a laboratory qualified (LQ) stress-reference specimen.

11.3.1.1 Manufacturing

The manufacturing process of the reference specimen shall insure a high homogeneity of microstructure and a time-constant value of stress.
A simple geometry of the specimen is recommended to insure quality of the measurement (flatness, low roughness, etc.). The stress level should be high enough to minimise errors in the measurement. A number of measurements should be performed by the laboratory on the goniometer which has been carefully aligned (see clause 6.4.1). The reference values σ_{ref}, τ_{ref} and L_{ref} of the specimen are defined as the averages of these results. The repeatability $r_{\sigma ref}$, $r_{\tau ref}$ and r_{Lref} are equal to 2.8 $s_{\sigma ref}$, 2.8 $s_{\tau ref}$, 2.8 $s_{Lref,}$ where $s_{\sigma ref}$, $s_{\tau ref,}$ and s_{Lref} are the standard deviations on σ_{ref}, τ_{ref} and L_{ref}.

11.3.1.2 Evaluation of characteristic parameters

The characteristic parameters are:

— the normal stress value σ_{ref} and its repeatability $r_{\sigma ref}$

— the shear stress value τ_{ref} and its repeatability $r_{\tau ref}$

— value of the average width L_{ref} and its repeatability $r_{Lref.}$

The values of these parameters are obtained according to the ISO 5725-1 standard.
The repeatability is obtained according to ISO 5725-2 standard and the values shall be recorded.

11.3.2 Inter-laboratory qualified (ILQ) stress-reference specimen

An inter-laboratory qualified (ILQ) stress-reference specimen is physically similar to LQ stress-reference specimens but shall be analysed by several laboratories in order to increase the chances of detecting systematic errors or improper measurement protocols.

It shall fulfil the basic assumptions of the standard method described in the present document: weak crystalline texture, fine grains, flat surface, low roughness, negligible stress or composition gradients in the depth and along the surface. Furthermore, the mechanical state shall be stable with time. The stress level should be as high as possible, at least $1/(500\,½\,S_2^{\{hkl\}})$

It is not necessary to know the chemical composition or the microstructure precisely. The reference values of the specimen: normal stress σ_{ref}, shear stress τ_{ref} and reproducibility R_σ, R_τ and repeatability r_σ, r_τ values can be obtained by inter-laboratory round robins involving at least 5 laboratories. Until certified specimens are

commercially available, groups of laboratory can be constituted freely in order to manufacture and characterise the specimens. Information on the organisation of inter-laboratory round robins can be found in ISO 5725-2 standard. The computation of repeatability and reproducibility is also described in ISO 5725-2 standard. These are defined as 2.8 s_r and 2.8 s_R where s_r and s_R are standard deviations of the repeatability and reproducibility respectively.

In the certificate of the specimen the reference values of the specimen shall be indicated along with the experimental conditions (lattice plane family, radiation, approximate spot size, location of the measurement area, the ψ values used, XECs, S_1 direction, oscillations or masking if any).

12 Limiting cases

12.1 Introduction

The limiting cases are:

— Stress gradients;

— Lattice constants gradient;

— Layer removal (see 5.2.2.1);

— Surface roughness;

— Non-flat surfaces (see 5.1.1);

— Highly textured materials;

— Coarse grain material (see 5.1.3);

— Multiphase materials;

— Overlapping diffraction lines;

— Broad diffraction lines.

12.2 Presence of a subsurface stress gradient

A strong stress gradient will lead to a curvature of the plot of the lattice spacing (or diffraction line position) versus $\sin^2\psi$ (see clause 8.4). This curvature is independent of the sign of the ψ values used.
If stress gradients are present, the X-ray diffraction measurement can be used for stress calculations only if:

$$\frac{\partial\sigma}{\partial Z} < \frac{1}{z} \cdot \frac{1}{1/2\, S_2^{hkl}} \cdot \frac{1}{500} \qquad (19)$$

where

$\frac{\partial\sigma}{\partial Z}$ the stress gradient with respect to the distance to the surface of the specimen

z penetration of the x-rays

$^1/_2S_2^{\{hkl\}}$ Elasticity constant of the family of lattice planes{hkl}

The penetration of x-rays can be calculated by formulae reported in clause 6.2

It is possible to correct the data for the errors caused by the penetration of the X-ray beam, if no depth measurements are performed and the stress profile is accurately calculated. To minimise gradient effects, and thus to improve the measurement quality, it is suggested:

— to reduce the X-ray penetration by using a more suitable wavelength,

— to choose a more suitable diffraction angle,

— to use low incidence angles.

12.3 Surface stress gradient

In several cases, regions with high plastic strains may be very confined (plastic strains around inclusions, cracks or holes, edges of laser treatment or welding, sharp contacts, etc.), and strong gradients are generated. Thus, in this case the residual stress evaluated by X-ray diffraction depends on the size and the position of the irradiated area and the assumption of uniform stress holds only if the irradiated area is sufficiently small. Indeed, if the stress values measured within an area are very different, choosing a large enough irradiated area may provide a useful "average" surface stress, even if large fluctuations of its local value are present. But, with the use of a too small diffracting area, an insufficient number of crystallites diffracts and the coarse grain diffraction difficulties may appear [7].

12.4 Surface roughness

12.5 Non-flat surfaces

Curved surfaces lead to too low absolute values of the stress.

The irradiated area should be smaller than 0.4 times the radius of curvature of the analysed surface in the direction of the stress component to be determined. Beyond this limit, corrections shall be performed [8,9].

12.6 Effects of specimen microstructure

12.6.1 Textured materials

Texture effects are moderate if the variations of integrated intensity over the whole set of the data fulfil:

$$\frac{\mathrm{Max}\, I_{\phi\psi}^{\{hkl\}}}{\mathrm{Min}\, I_{\phi\psi}^{\{hkl\}}} < 3 \qquad (19a)$$

where

I_{hkl} Net integrated intensity of the hkl diffraction line

Otherwise, two effects have to be considered:

— Elastic anisotropy: the relationship between stress and measured strains becomes:

$$\varepsilon_{\phi\psi} = \sum_{i,j=1\,\mathrm{to}\,3} F_{ij}\, \sigma_{ij}\,, \qquad (19b)$$

where

$\varepsilon_{\phi\psi}^{\{hkl\}}$ is the strain in the direction defined by the angles ϕ and ψ

F_{ij} are called Generalised XEC.

The F_{ij} depend on the Orientation Distribution Function of the material. They can be calculated or determined experimentally (For details see e.g. [10]).

— Plastic anisotropy: in addition to the effect of macroscopic stresses, the elastic strain of the diffracting volume contains a term $\varepsilon_{\phi\psi}^{m}$ related to the accommodation of the local plastic anisotropy:

- $\varepsilon_{\phi\psi} = F_{ij}\ \sigma_{ij} + \varepsilon^{m}_{\phi\psi}$. (19c)

The term $\varepsilon^{m}_{\phi\psi}$ can cause non-linearity in the $\varepsilon_{\phi\psi}$ vs. $\sin^2\psi$ plots. At this time there is no general method to handle the problem.

Measurements on several reflections taking an average of the stress values obtained or establishing the $\varepsilon_{\phi\psi}$-$\sin^2\psi$ curve from $\varepsilon_{\phi\psi}$ values obtained on different reflections may be used.

12.6.2 Multiphase materials

If several phases are present in the specimen, the calculated residual stresses can be attributed, as a first approximation, to the phase to which the chosen reflection belongs. When the phase is a small percentage or when its elastic-plastic behaviour is different from that of the pure material, the stress can be greatly different with respect to the macroscopic stress.
Usually, in these cases there are two ways to obtain the macroscopic stress:

- to measure the strains in all phases;
- to adopt other methods to evaluate the macroscopic stress (by strain gauge, etc...).

With the strains in all phases, the determination of macroscopic residual stresses may present several difficulties.
In a single phase material, with the domain size, shear stresses in the planes perpendicular to the specimen surface may be present ($\sigma_{13} \neq \sigma_{23} \neq 0$). In the same way, in multiphase materials, accommodation may induce $\sigma_{33} \neq 0$ in each phase, especially, when several phase transformations have occurred in the material.
So for the determination of the macroscopic stresses with the classical X-ray method applied on each phase the volume fraction and the free stress lattice spacing d_0 of each phase is required.

In multiphase materials if the grain size is smaller than the penetration depth of the X-rays, then the through thickness residual stress (σ_{33}) should be taken into account [more precise ref.10].

12.7 Broad diffraction lines

The position of broad diffraction lines is determined with low precision and systematic errors, which may arise from truncation effects.

In particular, problems can arise when:

— the line width is greater than 1/3 of the angular range of the measurement;

— the difference between the intensities after LP and absorption corrections on the right and left-hand side of the line is greater than 20% of the intensity of the maximum (see Figure 10).

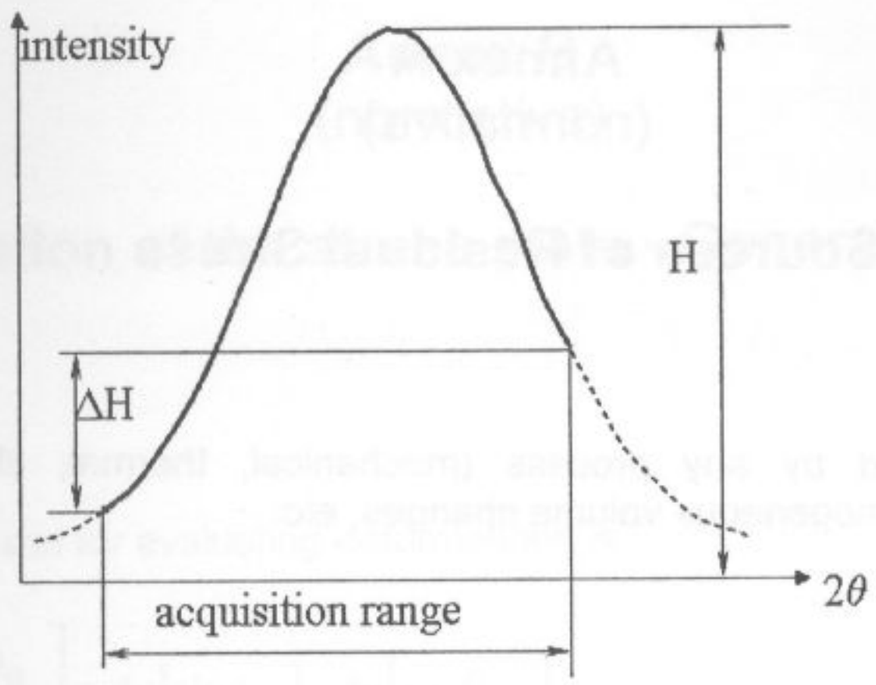

Key
H peak height
ΔH

Figure 10 — Example of a broad diffraction line that may cause problems of truncation because ΔH > 20% H

In these cases it is suggested:

— - to collect a wider 2θ range;

— - to change the {hkl} planes;

— - to optimise the diffraction line treatment.

Annex A
(normative)

Sources of Residual Stress

Residual stresses are generated by any process (mechanical, thermal, chemical), which leads to inhomogeneous deformation, inhomogeneous volume changes, etc.

A.1 Mechanical processes

— Surface treatments

— Drawing

— Rolling

— Grinding and mechanical polishing

— Machining

— Assembling

A.2 Thermal processes

Residual stresses may arise from thermal gradients as well as from phase transformations, e.g. in the case of heat-treated steel.
Examples: quenching, casting, butt welding, tempering, ageing, etc.

A.3 Chemical processes

Chemical processes, like oxidation, corrosion, electroplating, etc are sources of residual stress.

Annex B
(normative)

Determination of the stress state - General Procedure

B.1 General

The mathematical definition used for evaluating deformations is:

$$\varepsilon_{\phi\psi}^{\{hkl\}} = \ln\left[\frac{d_{\phi\psi}}{d_0}\right] = \ln\left[\frac{\sin\theta_0}{\sin\theta_{\phi\psi}}\right] = \ln[\sin\theta_0] - \ln[\sin\theta_{\phi\psi}] \qquad \text{(B.1)}$$

The general formula used for the stress tensor calculation in a triaxial stress state is:

$$\varepsilon_{\phi\psi}^{\{hkl\}} = \frac{1}{2}S_2^{\{hkl\}}.\left[\begin{matrix}\left(\sigma_{11}\cos^2\phi + \sigma_{22}\sin^2\phi + \tau_{12}\sin 2\phi - \sigma_{33}\right).\sin^2\psi \\ +\left(\tau_{13}\cos\phi + \tau_{23}\sin\phi\right).\sin 2\psi + \sigma_{33}\end{matrix}\right] + S_1^{\{hkl\}}.\mathrm{Tr}\left(\overline{\overline{\sigma}}\right) \qquad \text{(B.2)}$$

where for formulae (B.1) and (B.2)

$\varepsilon_{\phi\psi}^{\{hkl\}}$ is the strain in the direction defined by the angles ϕ and ψ for the family of lattice planes {hkl};

d_0 Interplanar distance (d spacing) of a strain free specimen.

$d_{\phi\psi}$ Interplanar distance (d spacing) of strained material in the direction of measurement defined by the angles ϕ and ψ.

θ_0 the Bragg angle associated to d_0

$\theta_{\phi\psi}$ the Bragg angle defined in the direction ϕ and ψ according to Bragg law (see EN13925-1, pag. 6)

$^1/_2S_2^{\{hkl\}}$ Elasticity constant of the family of lattice planes{hkl}

σ_{11}, σ_{22}, σ_{33} are normal stress components in the directions S_1, S_2 and S_3;

τ_{12} is the shear stress within the plane defined by S_1 and S_2;

τ_{13} is the shear stress within the plane defined by S_1 and S_3;

τ_{23} is the shear stress within the plane defined by S_2 and S_3.

$\mathrm{Tr}(\sigma)$ Trace of the stress tensor : $\mathrm{Tr}(\sigma) = \Sigma\sigma_{ii}$

Assuming $\sigma_{33} = 0$.

Combining these two relations, it is possible to define a procedure to calculate the stress tensor components.

Biaxial and uniaxial stress states are particular cases of the calculation. The procedures to calculate these stress states are the same, replacing some components σ_{ij} by a zero value.

B.2 Using the exact definition of the deformation

B.2.1 General

Replacing the exact definition of $\varepsilon_{\phi\psi}^{hkl}$ (B.1) in relation (B.2), we obtain an expression of Bragg angle θ values as a function of the stress state.

$$\ln[\sin\theta_{\phi\psi}] = \ln[\sin\theta_0] - \frac{1}{2}S_2^{\{hkl\}}\left[\begin{array}{l}(\sigma_{11}\cos^2\phi + \sigma_{22}\sin^2\phi + \tau_{12}\sin 2\phi)\sin^2\psi \\ +(\tau_{13}\cos\phi + \tau_{23}\sin\phi)\sin 2\psi\end{array}\right] - S_1^{\{hkl\}}Tr(\bar{\bar{\sigma}}) \qquad \text{(B.3)}$$

where

θ_0 the Bragg angle associated to d_0

$\theta_{\phi\psi}$ the Bragg angle defined in the direction ϕ and ψ according to Bragg law (see EN13925-1, pag. 6)

$^1/_2S_2^{\{hkl\}}$ Elasticity constant of the family of lattice planes{hkl}

σ_{11}, σ_{22}, σ_{33} are normal stress components in the directions S_1, S_2 and S_3;

τ_{12} is the shear stress within the plane defined by S_1 and S_2;

τ_{13} is the shear stress within the plane defined by S_1 and S_3;

τ_{23} is the shear stress within the plane defined by S_2 and S_3.

$Tr(\sigma)$ Trace of the stress tensor : $Tr(\sigma) = \Sigma\sigma_{ii}$

B.2.2 Determination of the stress tensor components

Using

— $a_{ij} = -\frac{1}{2}S_2^{\{hkl\}}\cdot\sigma_{ij}$ (B.4)

and

$$K = \ln[\sin\theta_0] - S_1^{\{hkl\}}.Tr(\bar{\bar{\sigma}}) \qquad \text{(B.5)}$$

and with (B.6)

$$f_{11} = \cos^2\phi\cdot\sin^2\psi;\quad f_{22} = \sin^2\phi\cdot\sin^2\psi;\quad f_{12} = \sin 2\phi\cdot\sin^2\psi\quad f_{13} = \cos\phi\cdot\sin 2\psi;\quad f_{23} = \sin\phi\cdot\sin 2\psi$$

relation (3) can be written :

— $\ln[\sin\theta_{\phi\psi}] = K + \sum_{i,j}^{3} f_{ij}.a_{ij}$ (B.7)

Knowing $\theta_{\phi\psi}$ values versus f_{ij} (5 functions of ψ and ϕ angles), we can determine the 5 a_{ij} constants values and the constant **K** value. Linear regression calculation is the most suitable tool for this determination.

Then, the stress is calculated by values which do not depend on θ_0 value:

$$\sigma_{ij} = -\frac{a_{ij}}{\frac{1}{2}S_2^{\{hkl\}}} \quad \text{(B.8)}$$

where the symbols in formulae (B.4), (B.5), (B.6), (B.7), (B.8) are:

σ_{ii} Normal stress components (i=1,2,3)

$^1/_2S_2^{\{hkl\}}$ Elasticity constant of the family of lattice planes{hkl}

$Tr(\sigma)$ Trace of the stress tensor : $Tr(\sigma) = \Sigma\sigma_{ii}$

$f_{11}, f_{22}, f_{12}, f_{13}, f_{23}$ are the strain coefficients

$\theta_{\phi\psi}$ the Bragg angle defined in the direction ϕ and ψ according to Bragg law (see EN13925-1, pag. 6).

B.2.3 Determination of θ and d_0

If

— $Tr\left(\overline{\overline{\sigma}}\right) = \sigma_{11} + \sigma_{22}$ is known, we can determine θ_0, using relation (5). From θ_0 d_0 is obtained using Bragg's law.

The determination of $Tr\left(\overline{\overline{\sigma}}\right)$ depends on the type of analysis.

This value cannot be determined from a single direction analysis. But, if we consider the stress tensor to be isotropic $(\sigma_{11} \approx \sigma_{22})$, we can write $Tr\left(\overline{\overline{\sigma}}\right) \approx 2 \cdot \sigma_{11}$.

This calculation is not necessary for the determination of stress tensor components, using the general definition of deformation.

B.3 Using an approximation of the definition of the deformation

B.3.1 General

For historical reasons, a deprecated approximation of the deformation definition may be used:

— $\varepsilon_{\phi\psi}^{hkl} = \frac{\theta_0 - \theta_{\phi\psi}}{\tan(\theta_0)}$ (B.9)

with $b_{ij} = \tan(\theta_0) \cdot a_{ij}$ (B.10)

and using the same notations as previously, one can write :

— $\theta_{\phi\psi} = K - \sum_{i,j}^{3} f_{ij} \cdot b_{ij}$ (B.11)

with $K = \theta_0 - S_1^{\{hkl\}} \cdot Tr\left(\overline{\overline{\sigma}}\right)$

B.3.2 Determination of the stress tensor components

Knowing $\theta_{\phi\psi}$ values versus f_{ij} (5 functions of ψ and ϕ angles), one can determine the 5 b_{ij} constants values and the constant **K** value. Linear regression calculation is the most suitable tool for this determination.

Then, stress tensor components are calculated with:

— $\sigma_{ij} = -\frac{b_{ij}}{\frac{1}{2} S_2^{\{hkl\}} . \tan(\theta_0)}$ (B.12)

These values depend on θ_0 value, which is necessary to calculate the stress tensor components.

This approach induces a systematic error in the stress values.

B.3.3 Determination of θ_0 and d_0

Sometimes, an approximation of this value is used, such as $\theta_{(sin^2\psi=0.4)}$. The definition of $\mathbf{Tr}\left(\overline{\overline{\sigma}}\right)$ implies:

$$K = \frac{S_1^{\{hkl\}}}{\frac{1}{2} S_2^{\{hkl\}} . \tan(\theta_0)} . (b_{11} + b_{22}) + \theta_0 \quad \text{(B.13)}$$

If at least two perpendicular directions are analysed, then the sum $b_{11} + b_{22}$ is known, and θ_0 can be determined resolving the equation (13) by iterative algorithm. (From θ_0 d_0 is obtained using Bragg's law.) If this is not the case, only $\mathbf{b_{11}}$ is known. But, if we may consider that the stress tensor is isotropic $(\sigma_{11} \approx \sigma_{22})$, we can write $\mathbf{b}_{22} \approx \mathbf{b}_{11}$.

This approach is more complex than the one presented in annex B.1 and is always an approximation of the exact θ_0 value. It is not to be used.

Annex C
(normative)

Recent developments

C.1 Stress measurement using two-dimensional diffraction data

If an area detector is used, the basic principle of the ω-tilt, χ- tilt or a combination of the two can be used. In order to make use of all the information from an area detector in a simple way, it is useful to define an angle γ. This angle γ is the azimuthal angle on the diffraction cone belonging to a {hkl} reflection as shown in Figure C.1

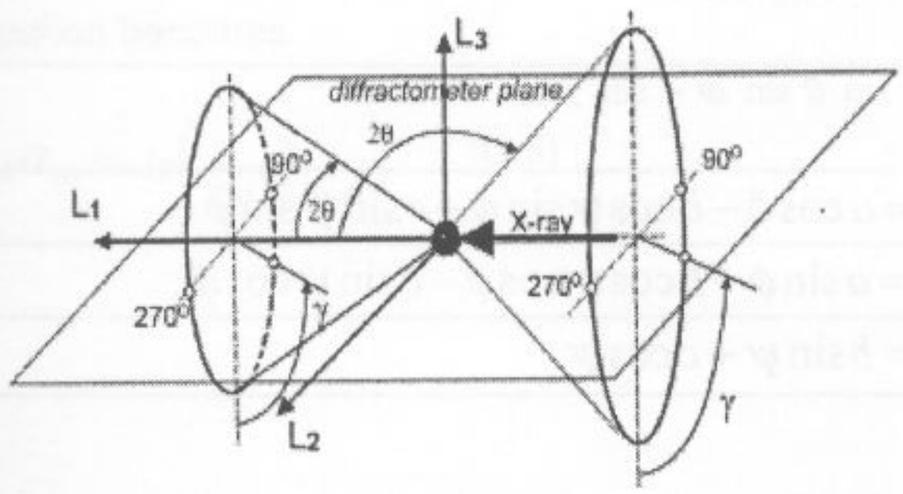

Key

L_1, L_2, L_3	Laboratory coordinate system
2θ	The diffraction angle, this is the angle between the incident and diffracted X-ray beams
X-ray arrow	the incident beam
γ	Azimuthal angle

Figure C.1 — The geometric definition of diffraction rings in laboratory axes.

The diffraction cone contains far more information than the part of the cone collected in a conventional one-dimensional measurement.

Diffraction cones from a stress-free polycrystalline specimen are regular cones in which the diffraction angle is constant. A stress in the specimen distorts the diffraction cones shape so that they are no longer regular cones. Then the diffraction angle becomes a function of γ, $2\theta(\gamma)$, and this function is uniquely determined by the stress tensor and the specimen orientation. This enables stress measurement. The benefit of the 2D method is that so many data points can be used to calculate stresses that results in a satisfactory measurement with short data collection time.

The relationship between strain tensor and diffraction cone distortion is defined by the fundamental equation [11]

— $f_{11}\varepsilon_{11} + f_{12}\varepsilon_{12} + f_{22}\varepsilon_{22} + f_{13}\varepsilon_{13} + f_{23}\varepsilon_{23} + f_{33}\varepsilon_{33} = \ln\left(\frac{\sin\theta_0}{\sin\theta}\right)$ (C.1)

where

ε_{ij}'s are the strain tensor components in the specimen coordinate system $S_1 S_2 S_3$,

f_{ij}'s are strain coefficients determined by the simplified equations in Table C.1

f_{11} =	f_{12} =	f_{22} =	f_{13} =	f_{23} =	f_{33} =
h_1^2	$2h_1h_2$	h_2^2	$2h_1h_3$	$2h_2h_3$	h_3^2
$a = \sin\theta\cos\omega + \sin\gamma\cos\theta\sin\omega$					
$b = -\cos\gamma\cos\theta$					
$c = \sin\theta\sin\omega - \sin\gamma\cos\theta\cos\omega$					
$h_1 = a\cos\phi - b\cos\psi\sin\phi + c\sin\psi\sin\phi$					
$h_2 = a\sin\phi + b\cos\psi\cos\phi - c\sin\psi\cos\phi$					
$h_3 = b\sin\psi + c\cos\psi$					

Table C.1 — Equations for Strain Coefficients f_{ij}

Where $\{h_1, h_2, h_3\}$ are the components of the unit vector of the diffraction vector $\mathbf{H}_{hkl}$ expressed in the specimen coordinates.

The stress tensor can be calculated from the strain tensor by using the general Hooke's law

— $\sigma_{ij} = C_{ijkl}\varepsilon_{kl}$ (C.2)

where

σ_{ij} stress tensor

C_{ijkl} represent the elastic stiffness coefficients in the specimen coordinates. For isotropic materials, there are only two independent elastic constants, , $S_1^{\{hkl\}}$ and $1/2S_2^{\{hkl\}}$.

We have the equation for stresses:

— $p_{11}\sigma_{11} + p_{12}\sigma_{12} + p_{13}\sigma_{13} + p_{22}\sigma_{22} + p_{23}\sigma_{23} + p_{33}\sigma_{33} = \ln\left(\frac{\sin\theta_0}{\sin\theta}\right)$ (C.3)

where

P_{ij}'s are stress coefficients

$$p_{ij} = \begin{cases} = \frac{1}{2} S_2^{\{hkl\}} f_{ij} + S_1 & \text{if } i = j \\ = \frac{1}{2} S_2^{\{hkl\}} f_{ij} & \text{if } i \neq j \end{cases} \quad \text{(C.4)}$$

$\ln(\sin\theta_0/\sin\theta)$ determines the diffraction cone distortion at each γ angle which is determined by the measured function $2\theta(\gamma)$ for a particular specimen orientation (ω, ψ, ϕ).

The following alternative expressions can be used for the diffraction cone distortion term.

$$\ln\left(\frac{\sin\theta_0}{\sin\theta}\right) = \ln\left(\frac{\lambda}{2d_0\sin\theta}\right)$$

Each diffraction frame corresponds to one specimen orientation (ω, ψ and ϕ). The diffraction ring on each frame is integrated and peak-fitted over a selected number of sections along the ring, so as to obtain a set of (χ, 2θ) data points representing the $2\theta(\chi)$ function. The stress tensor can be determined by fitting the data points to equation (3) with the least-squares method.

For biaxial stress, the above equation becomes

$$p_{11}\sigma_{11} + p_{12}\sigma_{12} + p_{22}\sigma_{22} + p_{ph}\sigma_{ph} = \ln\left(\frac{\lambda}{2d_0'\sin\theta}\right) \quad \text{(C.5)}$$

where

$$p_{ph} = \frac{1}{2} S_2^{\{hkl\}} + 3 S_1^{\{hkl\}},$$

σ_{ph} is a pseudo hydrostatic stress component caused by the approximated-spacing d_0'.

For biaxial stress with shear, we have

$$p_{11}\sigma_{11} + p_{12}\sigma_{12} + p_{22}\sigma_{22} + p_{13}\sigma_{13} + p_{23}\sigma_{23} + p_{ph}\sigma_{ph} = \ln\left(\frac{\lambda}{2d_0'\sin\theta}\right) \quad \text{(C.6)}$$

The biaxial stress state (equation 5) corresponds to the straight line of the ***d***-$\sin^2\psi$ plot. And the biaxial stress with shear (equation 6) is the case when there is a split between the data points in $+\psi$ side and $-\psi$ side. The general normal stress (σ_ϕ) and shear stress (τ_ϕ) at any arbitrary given ϕ angle are given by

$$\sigma_\phi = \sigma_{11}\cos^2\phi + \sigma_{12}\sin 2\phi + \sigma_{22}\sin^2\phi \quad \text{(C.7)}$$

$$\tau_\phi = \sigma_{13}\cos\phi + \sigma_{23}\sin\phi \quad \text{(C.8)}$$

In the Biaxial (2D) and Biaxial + Shear (2D) calculation, it is assumed that σ_{33} is zero so that we can calculate stress with an approximation of d_0 (or $2\theta_0$). Any error in d_0 (or $2\theta_0$) contributes only to a pseudo-hydrostatic term σ_{ph}. If we use d_0' to represent the initial input, then the true d_0 (or $2\theta_0$) can be calculated from σ_{ph} with the following equations:

$$d_0 = d_0' \exp(\ p_{ph}\ \sigma_{ph}\ ) \quad \text{(C.9)}$$

or

$$\theta_0 = \arcsin\ \left[\sin\ \theta_0' \exp(\ -\ p_{ph}\ \sigma_{ph}\ )\right] \quad \text{(C.10)}$$

C.2 Depth resolved evaluation of near surface residual stress - The Scattering Vector Method

The scattering vector method [12, 13] is a special X-ray stress analysis (XSA) technique that was developed for the
depth resolved evaluation of near surface residual stress fields. In contrast to the $\sin^2\psi$- based XSA methods, where the penetration depth z is adjusted by the variation of the inclination angle ψ between the surface normal and the diffraction vector $\boldsymbol{g}_{hkl}$, the scattering vector method is based on strain depth profiling by a specimen rotation η around $\boldsymbol{g}_{hkl}$ at fixed orientations (ϕ,ψ) of the diffraction vector with respect to the specimen system. The z -range covered by this rotation corresponds to the difference $\Delta z = z_\chi - z_\omega$ between the penetration depths of the χ-and the ω-method of the conventional XSA.

Because ψ is kept fixed during depth profiling in the 'scattering vector-' or 'η' method, the individual stress tensor depth profiles $\sigma_{ij}(z)$, which are coupled in the fundamental equation of the XSA, can be analysed separately.
The evaluation method is based on the extreme sensitivity of the individual strain profiles $\varepsilon_{\varphi\psi}(hkl, z)$ with respect to
the strain-free lattice spacing $d_0(hkl)$, which can be used as a criterion for a simultaneous determination of $d_0(hkl)$
itself as well as of the $\sigma_{ij}(z)$- profiles.

Therefore, the scattering vector method can be applied to analyse both, biaxial and triaxial residual stress fields in the near surface zone of polycrystalline materials. In the latter case it yields self-consistently the depth profiles of the in-plane stresses, $\sigma_{11}(z)$ and $\sigma_{22}(z)$, of the stress component $\sigma_{33}(z)$ normal to the surface, as well as
the strain-free lattice spacing $d_0(hkl)$. It should be stressed that the method has special preferences for the analysis
of residual stress gradients in strongly textured thin films, because in this case depth profiling can be performed in
the intensity poles of the texture and/or at grazing incidence.

C.3 Accuracy improvement through the use of equilibrium conditions for determination of stress profile

The residual stress fields are linked to incompatible strains generated by inhomogeneous plastic deformation and are self-balanced over the tested piece and should satisfy the equilibrium equations. So, the tension and the compression existing at the different points (or depths) of the specimen are not independent one of the other. The whole set of X-rays diffraction data acquired for different points and inclinations (Φ,Ψ) can be considered as a one single statistical sampling, and the residual stress and strain profiles can be determined by a global stress evaluation method [15].

That global method offers several advantages:

i) the errors bars of the evaluated stress profile are greatly reduced;

ii) for mechanical resistance approach, that global strain profile determination is the only way for getting the residual stress fields in F.E.M code;

iii) several elements of the residual-stress generation process and elasto-plastic behaviour can be identified;

iv) in the case of a depth profile, the stress redistribution due to the layer removal is taken into account directly.

Annex D
(normative)

Details of treatment of the measured data

D.1 Intensity correction on the scan

For the intensity correction the order of corrections shall be reported. The recommended order is:

1) Divergence slit conversion,

2) Absorption,

3) Background removal,

4) Lorentz-Polarisation,

5) K-α_2 Stripping.

The corrections are treated here as modifications on the raw data in the traditional way. Alternatively, in a more modern way, the corrections (e.g. background and K-Alpha2) can be included in the calculation of profile functions that are fitted to the raw data in order to determine the diffraction line position.

In the report, all the performed correction steps shall be reported and the omitted corrections should be mentioned too.

D.1.1 Divergence slit conversion

In Bragg Brentano geometry diffraction patterns are usually recorded using a fixed equatorial divergence slit. In this case the irradiated area decreases with decreasing diffraction angle. If it is preferred to have a constant irradiated area, e.g. to ensure that the X-ray beam does not overflow the specimen for all applied angles, then automatic divergence slits can be used. In data evaluation programs it is usually assumed that the intensities are measured in Bragg Brentano geometry using a fixed equatorial divergence slit. Consequently, intensities measured with automatic divergence slits shall be converted to values as if they were measured with fixed divergence slits under the assumption that the X-ray beam does not overflow the area of the specimen surface to be probed for all applied angles. This conversion is called a divergence slit conversion.

The conversion formula is

$$I_{FDS} = C_{div} I_{ADS} \qquad \text{(D.1a)}$$

where:

I_{FDS} = corrected intensity as if measured with Fixed Divergence Slit,

C_{div}= divergence slit correction factor,

I_{ADS} = measured intensity with Automatic Divergence Slit.

The correction factor C_{div} shall be re-evaluated for each measured intensity point.

If beam overflow occurs intensity corrections are possible, but give only approximate values. Beam overflow should be avoided if possible.

D.1.1.1 ω method

In the ω method the intensities are usually measured with a fixed equatorial divergence slit and need no correction.

$$C_{div} = 1 \qquad \text{(D.1b)}$$

In case automatic equatorial divergence slits are applied without beam overflow the intensities shall be converted to fixed slits intensities.

$$C_{div} = 2R\frac{\tan(\frac{1}{2}\delta_{FDS})}{L_{ADS}\sin\omega} \qquad \text{(D.1c)}$$

where

R = radius goniometer,

δ_{FDS} = fixed divergence slit angle (full angular range),

L_{ADS} = irradiated length,

ω = angle of incidence.

D.1.1.2 χ method

In the χ method, the intensities are usually measured with a fixed axial divergence slit and need no correction.

$$C_{div} = 1 \qquad \text{(D1d)}$$

Automatic slits are not common with the χ method. In case automatic axial divergence slits are applied without beam overflow the intensities shall be converted to fixed slits intensities in an appropriate way.

D.1.2 Absorption correction

For the absorption correction the intensities are assumed to be valid for fixed divergence slits (measured or corrected) and measured on a thick specimen. For a thick specimen the X-ray beam is fully absorbed by the analysed part for all applied angles. This condition is adequately fulfilled when the thickness of the analysed part is at least twice the average information depth, z, as calculated for a thick specimen (see Eqs 9b or 9d).

The correction formula is

$$I_{Abs-corr} = \frac{I_{FDS}}{A} \qquad \text{(D.2a)}$$

Where

I_{FDS} = corrected intensity as if measured with Fixed Divergence Slit,

A= absorption correction factor.

The absorption correction factor A shall be re-evaluated for each measured intensity point.

If for a thin specimen partial absorption of the X-ray beam occurs the intensities shall be corrected in an appropriate way.

D.1.2.1 ω method

For thick specimens the correction factor is:

$$A = 1 - \frac{\tan(\omega - \theta)}{\tan\theta} \qquad \text{(D.2b)}$$

where

θ = half of diffraction angle

(ω-θ) = ω-offset angle.

D.1.2.2 χ method

For thick specimens the correction factor is:

$$A = 1 \qquad \text{(D.2c)}$$

D.1.3 Background correction

The background is subtracted with:

$$I_{Bkg-corr} = I_{meas} - I_{bkg} \qquad \text{(D.3)}$$

where

I_{bkg} can be (a) horizontal background (slope = zero)

(b) linear background (slope and offset).

The background function is fitted to a number of intensity data points at the extremes of the measurement range.

The background function fitted and the numbers of intensity data points fitted shall be reported.

The type of background correction should be mentioned (constant background, linear background, spline approximation…).

D.1.4 Lorentz-polarisation correction

The combined correction for Lorentz and polarisation assumes that the specimen is a polycrystalline material with random orientation of the crystallites.

The correction formula for the Lorentz-polarisation factor *LP* is:

$$I_{LP-corr} = \frac{I_{meas}}{LP} \qquad \text{(D.4a)}$$

where

LP is the combined Lorentz-polarisation factor.

The Lorentz-polarisation factor *LP* shall be re-evaluated for each measured intensity point.

$$LP = \frac{1 + P_{mon} \cos^2 2\theta}{\sin^2 \theta \cos \theta} \qquad \text{(D.4b)}$$

In the above formulas P_{mon} describes the extra polarisation owing to the use of a monochromator (in incident or diffracted beam):

$$P_{mon} = \cos^2 2\theta_{mon} \qquad \text{(D.4c)}$$

where

$2\theta_{mon}$ = diffraction angle of the monochromator.

If no monochromator is used then

$$P_{mon} = 1 \qquad \text{(D.4d)}$$

The LP factor used and the value for P_{mon} shall be reported.

The above combined LP factor holds for diffraction peaks with a low structural broadening, which is not common in the practice of residual stress analysis. According to Warren& Averbach (1950) referenced by Delhez, Keijser, Mittemeijer and Rozendaal (1977) the LP factor for profiles with a significant structural broadening should be:

$$\text{LP} = \frac{1 + P_{mon} \cos^2 2\theta}{\sin^2 \theta}$$

This last formula should be used for the stress analysis.

D.1.5 K-Alpha2 stripping

The pure K-Alpha1 diffraction pattern is obtained from a K-Alpha1+K-Alpha2 diffraction pattern by means of a numerical K-Alpha2 stripping procedure. The doublet separation, δ_R, should be calculated as a 2θ dependent parameter. See formulae below:

$$I_{\alpha 2}(2\theta) = R_{\text{int}} I_{\alpha 1}(2\theta - \delta_R) \qquad \text{(D.5a)}$$

where

$$R_{\text{int}} \approx 0.5 \qquad \text{(D.5b)}$$

$$\delta_R = 2 \arcsin(R_{wav} \sin \theta_{\alpha 1}) - 2\theta_{\alpha 1} \qquad \text{(D.5c)}$$

$$R_{wav} = \frac{\lambda_{\alpha 2}}{\lambda_{\alpha 1}} \qquad \text{(D.5d)}$$

The value of R_{int} used shall be reported.

Alpha2 stripping should not be performed if it introduces instabilities in the treatment program, in particular if there is not enough background available on each side of the line.

D.2 Diffraction line position determination

D.2.1 Centre of Gravity methods

D.2.1.1 Classical Centre of Gravity

The centre of gravity (also called centroid) is calculated to determine the diffraction line position. The centroid of the profile $<2\theta>$ above a threshold value is defined as:

$$<2\theta>=\frac{\sum_{i=2\theta\_\min}^{2\theta\_\max} 2\theta_i I_i(2\theta_i)}{\sum_{i=2\theta\_\min}^{2\theta\_\max} I_i(2\theta_i)} \qquad \text{(D.6)}$$

where

2θ The diffraction angle, this is the angle between the incident and diffracted X-ray beams

I(x) is the net intensity

The threshold value is given as a percentage of the net peak height (i.e. peak height after subtraction of the background) and marks the starting angle and the end angle at each side of the peak. A too low threshold makes the method unstable. The recommended threshold is 20%.

D.2.1.2 Centred Centre of Gravity

This is a variant of the classical centre of gravity method.

The iterative sliding centre of gravity method calculates the centre of gravity position using intensities within an angular range. After the first calculation this range, in terms of a range in 2θ, is centred on the diffraction line position found in the first step and calculates a new centre of gravity. This step is repeated in an iterative way until the diffraction line position does not change any more according to a given accuracy value. The initial angular range is given in terms of an intensity threshold. A too low threshold makes this method unstable. The recommended initial threshold is 20%.

D.2.1.3 Sliding Centre of Gravity

This is another variant of the classical centre of gravity method. The iterative Sliding Centre of Gravity method calculates the centre of gravity positions using intensities thresholds between 20% and 80%. For each Threshold a
stress value as well as a corresponding standard deviation is calculated. In a second run, the centre of gravity positions are weighted with the standard deviation of the corresponding stress value and averaged. From the final
centre of gravity positions a final stress value is calculated.
This method allows to easily detect doubtful measurement and calculation conditions as those conditions generally cause a large standard deviation of the stress value or a systematic dependency of the stress values from the intensity threshold. In addition the method provides the automatic refinement of the evaluation parameters from a statistical point of view [14].

D.2.2 Parabola Fit

The 3-point parabola fit is not recommended.

It is recommended that the parabola function is fit to intensity data points above 85% of the maximum intensity with a minimum of 5 points.

D.2.3 Profile Function Fit

The definitions of the profile functions are given in prEN 13925-2 "Procedures" Annex D.

When using a fitting procedure, it shall be remembered that the more parameters are used, the better the line description but the greater the risks of instability of the algorithm. Stability problems shall be thoroughly investigated.

It is recommended to fit a residual background contribution simultaneously with the profile function.

It is recommended to disable the following fit parameters when they show unstable behaviour: slope of residual background contribution, asymmetry parameter, and profile shape parameter. In case the profile shape parameter of the PearsonVII or Pseudo-Voigt function behaves unstable then it is recommended to use the best fitting profile function with a fixed shape: Gauss, Lorentz, Modified Lorentz, or Intermediate Lorentz.

D.2.4 Middle of width at x% height method

The width of the diffraction line is determined at x% height of the peak maximum. Straight lines are fitted to the left and right flank of the peak to determine the width. A smoothing by a sliding polynomial (Stavitsky-Golay…) can also be used. The midpoint of the width is taken as the diffraction line position. The most commonly used method determines the midpoint of the FWHM (x=50%). Another common variant uses 2/3 of the height (x=67%). Other variants are also possible.

D.2.5 Cross-correlation method

The diffraction line position of a diffraction line (I_j) is given relatively to a reference diffraction line (I_{ref}). It is recommended to use the strongest line of a series of stress measurements as reference line. The cross-correlation function is defined as:

$$F_{ref,j}(\Delta 2\theta) = \int I_{ref}(2\theta) I_j(\Delta 2\theta - 2\theta) d(2\theta) \qquad \text{(D.7a)}$$

where the maximum of the function $F_{ref,j}(\Delta 2\theta)$ gives the diffraction line shift $\Delta 2\theta_{ref,j}$. The function $F_{ref,j}(\Delta 2\theta)$ is evaluated for all measurement points of the evaluated diffraction line (I_j) above an intensity threshold. The recommended threshold is 20% of the net maximum intensity.

The cross-correlation method gives diffraction line shifts only. It is recommended to evaluate the absolute position of the reference diffraction line with one of the other diffraction line determination methods.

Then the diffraction line position of diffraction line I_j is:

$$2\theta_j = 2\theta_{ref} + \Delta 2\theta_{j,\max} \qquad \text{(D.7b)}$$

The method used to determine the diffraction line position of the reference diffraction line shall be reported unambiguously, together with the function fitted (if any) and the values of the parameters implied.

D.3 Correction on the diffraction line position

The diffraction line positions can be optionally corrected for diffraction line shifts caused by remaining misalignments or the transparency effects. The corrections can be performed on the basis of measured diffraction line shifts or on the basis of calculated diffraction line shifts. The order of the corrections is not relevant. The applied corrections shall be reported.

D.3.1 Remaining misalignments

The diffraction line shifts due to small remaining misalignments shall be measured on a stress-free reference specimen. The corrections can be applied on the basis of measured diffraction line shifts or on the basis of calculated diffraction line shifts.

Two misalignment errors are relevant in analysing residual stress measurements: specimen displacement and incident beam misalignment (equatorial for ω-method and axial for χ-method).

The corrections shall be applied on the diffraction line positions according to the formula:

$$2\theta_{\text{corr}} = 2\theta_{\text{meas}} - \Delta 2\theta_{\text{sp}} - \Delta 2\theta_{\text{eq}} - \Delta 2\theta_{\text{ax}}\,, \tag{D8}$$

with for the ω-method:

$$\Delta 2\theta_{sp} = \frac{180}{\pi}\frac{2h_{\text{sp},\omega}}{R}\frac{\sin\theta}{\sin\omega}\cos\theta \tag{D8a}$$

$$\Delta 2\theta_{eq} = \frac{180}{\pi}\frac{2h_{\text{eq}}}{R}\frac{\sin(\omega-\theta)}{\sin\omega}\cos\theta \tag{D8b}$$

$$\Delta 2\theta_{ax} = 0 \tag{D8c}$$

and for the χ-method:

$$\Delta 2\theta_{sp} = \frac{180}{\pi}\frac{2h_{\text{sp},\chi}}{R}\frac{1}{\cos(\chi)}\cos\theta \tag{D8d}$$

$$\Delta 2\theta_{eq} = 0 \tag{D8e}$$

$$\Delta 2\theta_{ax} = \frac{180}{\pi}\frac{2h_{\text{ax}}}{R}\frac{\sin\chi}{\cos(\chi)}\cos\theta \tag{D8f}$$

where

$2\theta_{corr}$ = corrected diffraction line position

$2\theta_{meas}$ = measured diffraction line position

$\Delta 2\theta_{sp}$= specimen displacement

$\Delta 2\theta_{eq}$= equatorial beam misalignment (only for ω-method)

$\Delta 2\theta_{ax}$= axial beam misalignment (only for χ - method).

D.3.2 Transparency correction

The diffraction line shift due to the transparency effect is usually calculated. It requires first the calculation of the information depth (=weighted mean penetration depth) for each tilt.

The correction shall be applied on the diffraction line positions for each diffraction line according to the formula:

$$2\theta_{\text{corr}} = 2\theta_{\text{meas}} - \Delta 2\theta_{\text{tr}}\,, \tag{D.9a}$$

D.3.2.1 ωmethod

For thick specimens the information depth is:

$$z = \frac{\sin^2\theta - \sin^2(\omega-\theta)}{2\mu\sin\theta\cos(\omega-\theta)} \tag{D9b}$$

Then the diffraction line shift (in degrees) is:

$$\Delta 2\theta_{tr} = \frac{-180}{\pi}\frac{2z}{\mathrm{R}}\frac{\sin(\theta)\cos(\theta)}{\sin\omega} \qquad \text{(D9c)}$$

where

μ linear attenuation coefficient,

θ Bragg angle, this is the angle between the diffracting lattice planes and the incident beam.

$(\omega\text{-}\theta)$ offset angle,

z information depth,

R diffractometer radius.

D.3.2.2 χ method

For thick specimens the information depth is:

$$z = \frac{\sin\theta\cos\chi}{2\mu} \qquad \text{(D.9d)}$$

Then the diffraction line shift is:

$$\Delta 2\theta_{tr} = \frac{-180}{\pi}\frac{2z}{\mathrm{R}}\frac{\cos\theta}{\cos\chi} \qquad \text{(D.9e)}$$

where

μ linear attenuation coefficient,

θ Bragg angle, this is the angle between the diffracting lattice planes and the incident beam

χ tilt angle,

z information depth,

R diffractometer radius.

The transparency correction is usually negligible. It plays a role when the linear absorption coefficient, μ, is smaller than 200 cm^{-1}. For ceramics, oxides, light metals and polymers using Cr, Co or Cu radiation this is the case and for metals and hard metals too when Mo radiation is used.

Annex E
(informative)

General description of acquisition methods

E.1 Introduction

In the main text of the normative, only three acquisition methods are described, the ω method, the χ method and the modified χ method. The two first because they are widespread in both industrial and university laboratories and the third one because it is often used on portable goniometers. However, other methods exist that can be used for specific purposes. The aim of the present annex is to provide a general description of acquisition methods followed by applications to various methods used for X-ray stress analysis.

An acquisition method is defined by the set of orientations taken by the specimen with regard to the incident beam and the diffracted beams during the acquisition. The orientation of a solid is defined by a set of three angles that correspond to its three rotational degrees of freedom.

In X-ray stress analysis, the most fundamental set of three angles is (Φ, Ψ, η) where Φ and Ψ define the measurement direction $\vec{n}$ and η is a rotation angle around $\vec{n}$. However, this set of angle is not always convenient because, in general, they do not correspond to the angles of the goniometer. The purpose of the present annex is to give the relation between the two sets of angles in the case of a Euler cradle using the angles (φ, χ, ω). A similar approach can be given for any other kind of cradle such as a kappa cradle.

E.2 Definitions

Two orthonormal reference systems are defined :

The first one, called specimen reference system, is noted by : $(\vec{S}_1, \vec{S}_2, \vec{S}_3)$

- $\vec{S}_3$ is taken normal to the surface of the specimen and directed towards the outside
- $\vec{S}_1$ is in the plane of the surface and freely chosen by the operator. It is customary to choose it parallel to a physically meaningful direction such as the rolling direction, the machining direction, the welding direction,etc.
- $\vec{S}_2$ is taken so that the $(\vec{S}_1, \vec{S}_2, \vec{S}_3)$ system is direct.
- If the surface of the specimen is curved, the system is chosen with respect to the tangent plane at the point of measurement.

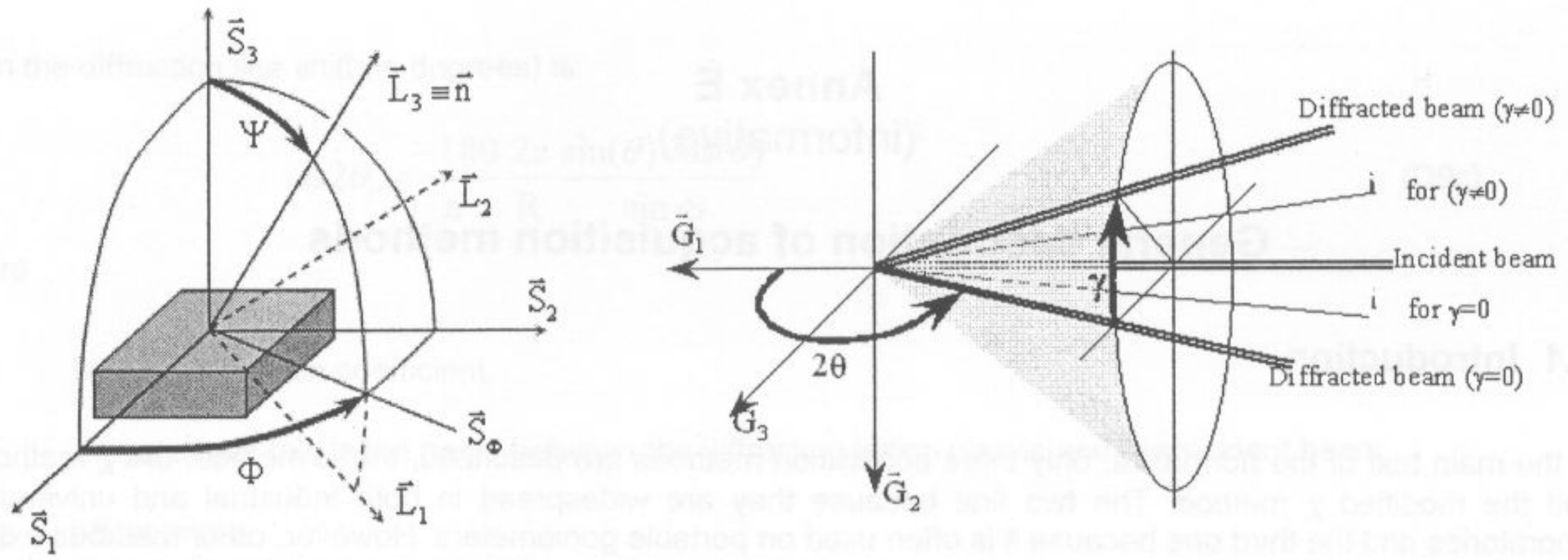

Key

S_1, S_2, S_3	Specimen coordinate system.
L_1, L_2, L_3	Laboratory coordinate system.
Φ	The angle between a fixed direction in the plane of the specimen and the projection in that plane of the normal to the diffracting planes.
Ψ	The angle between the normal of the specimen and the normal of the diffracting planes.

Figure E.1 — Definition of the specimen reference system and of the extensimetric angles Ψ, Φ (left). Definition of the diffraction angles 2θ and γ (right).

(note: Figure E1 (left) is equivalent to Figure 1 in the text of the of the body of the document. It should be omitted. If it is retained, the symbols shall be the same as for the text in the body of the standard. In particular the symbol Φ instead of ϕ can be misleading. If they have a different meaning such a meaning shall be defined.

The second one, called the goniometer reference system, is noted by : $(\vec{G}_1, \vec{G}_2, \vec{G}_3)$

- $\vec{G}_1$ is taken parallel to the incident X-ray beam and directed in the propagation direction of the photons
- $\vec{G}_2$ is taken parallel to the axial direction of the goniometer
- $\vec{G}_3$ is taken so that the $(\vec{G}_1, \vec{G}_2, \vec{G}_3)$ system is direct.

In the reference (starting) position, the two systems are superposed. The data acquisition is defined completely by the orientation of the two systems. Three groups of angles can be defined :

The first group is called the sampling angles, noted Φ, Ψ, η (capital phi, psi, eta) and is related to the mechanical state of the specimen at a given penetration depth. These angles define completely the orientation of the specimen and are useful if one works in the system $(\vec{S}_1, \vec{S}_2, \vec{S}_3)$.

- Φ and Ψ are the extensometric angles and they are called respectively azimuth and tilt angles. They define, in the system $(\vec{S}_1, \vec{S}_2, \vec{S}_3)$, the direction of measurement of the elastic strain $\varepsilon_{\Phi\Psi}$. This direction is described by a unit vector noted $\vec{n}$. For a given crystallographic plane family, Φ and Ψ enable to sample different crystallites that produce the diffraction peak.
- η defines a rotation around $\vec{n}$. A variation of η will cause a variation of the penetration depth (information depth). It will also cause a variation of $\varepsilon_{\Phi\Psi}$ only if there are stress gradients along the depth of the specimen. For given diffraction conditions and extensometric angles, η

enables to sample different depths below the surface of the specimen.

The second group is called the 3 goniometer angles φ, χ, ω (small phi, chi, omega) and they are used to orientate the specimen on the goniometer, they are useful if one works in the system $\left(\vec{G}_1, \vec{G}_2, \vec{G}_3\right)$. From the reference position, the specimen is brought into its measurement orientation by three successive rotations. It should be noticed that the order of the three rotations is important.

- A rotation by φ around $-\vec{G}_3$
- A rotation by χ around $\vec{G}_1$
- A rotation by ω around $-\vec{G}_2$

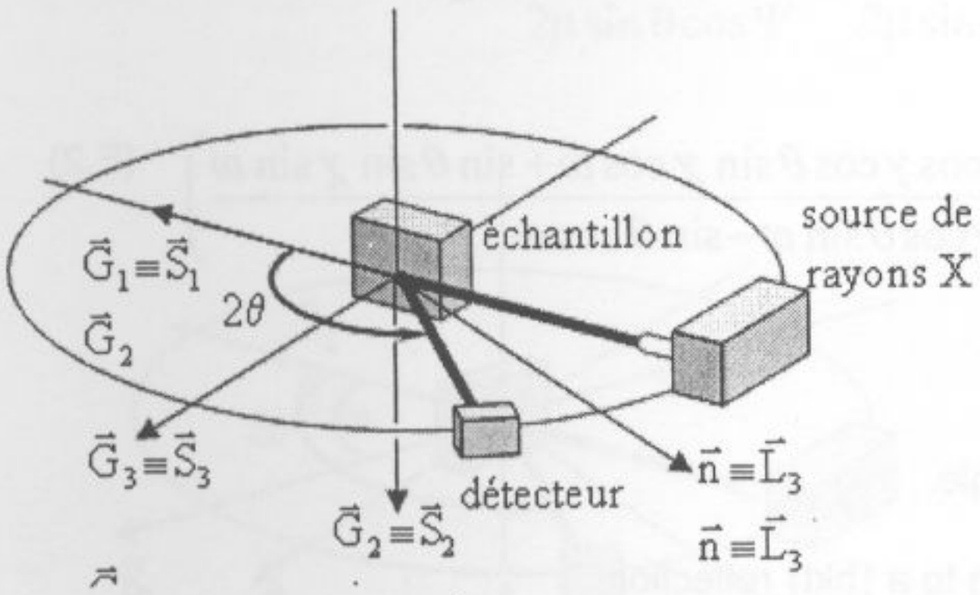

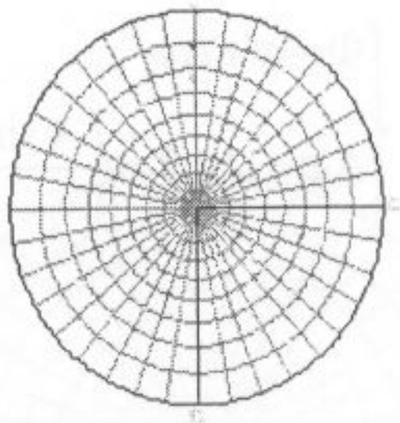

Key

$\left(\vec{S}_1, \vec{S}_2, \vec{S}_3\right)$	reference system
X	The incident beam
open circle	diffracted beam
black dot	bisector of the two beams

Figure E.2 - Reference position ($\chi = \varphi = \omega = 0$) the incident beam is parallel to the surface of the specimen and the two reference systems $\left(\vec{S}_1, \vec{S}_2, \vec{S}_3\right)$ and $\left(\vec{G}_1, \vec{G}_2, \vec{G}_3\right)$ are superposed. Perspective drawing (left) and stereographic representation for $2\theta = 156°$ (right).

Note: The caption should be modified and the explaining part of the caption put in texts

The third group is called the diffractometric angles θ and γ (theta, gamma) and they define the direction of the diffracted beam :

- θ is called the Bragg angle and the angle between the incident beam and the diffracted beam is 2θ.
- In a polycrystalline specimen, the diffracted beams form a cone of axis $\vec{G}_1$ and γ defines the position of one diffracted beam in the cone. The measurement direction is the bisector of the incident and diffracted beams.

In the following section, an acquisition method is described by giving the expressions of Ψ and Φ as a function of the goniometer angles (φ, χ, ω) and of the diffraction angles (θ, γ). The expressions of the penetration depth is given as a function of the diffraction angles and either with the sampling angles (η, Ψ, θ, γ) or with the goniometer angles (χ,ω, θ, γ). It can be noted that the penetration depth does not depend on angles φ or Φ for a specimen with a flat surface.

A particular acquisition method is obtained from the general method by setting some angles at a given fixed value.

E.3 Description of the various acquisition methods

E.3.1 General method

The expressions of Ψ and Φ are :

$$\Psi = \mathrm{ArcCos}(\cos\gamma\cos\theta\cos\chi\cos\omega + \sin\gamma\cos\theta\sin\chi + \sin\theta\cos\chi\sin\omega) \qquad \text{(E.1)}$$

and :

$$\begin{cases} \Phi = \varphi + \Delta\varphi \\ \Delta\varphi = ArcTan\left(\dfrac{-\sin\gamma\cos\theta\cos\chi + \cos\gamma\cos\theta\sin\chi\cos\omega + \sin\theta\sin\chi\sin\omega}{\cos\gamma\cos\theta\sin\omega - \sin\theta\cos\omega}\right) \end{cases} \qquad \text{(E.2)}$$

where:

Φ and Ψ are respectively the azimuth angle, the tilt angle.

γ is the azimuthal angle on the diffraction cone belonging to a {hkl} reflection.

θ is the Bragg angle

χ is the specimen orientation in the direction $\vec{G}_1$.

ω is the specimen orietation in the direction $-\vec{G}_2$.

φ is the specimen orientation in the direction $-\vec{G}_3$ of the goniometer system.

$\Delta\varphi$

All the acquisition modes with a 0D (punctual) or 1D (position sensitive) detector can be described by $\gamma = 0$. When a 2D detector is used, angle γ is necessary to describe the variations of Φ and Ψ along the portion of the Debye ring captured by the detector. The penetration depth can be given with the sampling angles :

$$z = \frac{\cos^2\Psi\sin^2\theta - \sin^2\Psi\cos^2\theta\sin^2\eta}{2\mu\sin\theta\cos\Psi} \qquad \text{(E.3)}$$

or with the goniometer angles :

$$z = \frac{\cos\chi\sin\omega}{\mu}\left[\frac{\sin 2\theta\cos\gamma\cos\chi\cos\omega + \sin 2\theta\sin\gamma\sin\chi - \cos 2\theta\cos\chi\sin\omega}{\sin 2\theta\cos\gamma\cos\chi\cos\omega + \sin 2\theta\sin\gamma\sin\chi - \cos 2\theta\cos\chi\sin\omega + \cos\chi\sin\omega}\right] \qquad \text{(E.4)}$$

Where

z is the penetration depth.

E.3.2 Omega (ω) method

This is an acquisition mode that can be achieved with a basic 2 circles (ω ; 2θ) powder diffractometer and a 0D or 1D detector. In this case $\gamma = 0$, $\chi = 0$ and $\eta = \pi/2$. From formulae (E.1) to (E.4), it gives :

$$\begin{cases} \Psi = \omega - \theta \\ \Phi = \varphi \end{cases} \tag{E.5}$$

with a penetration depth :

$$z = \frac{\sin^2\theta - \sin^2\Psi}{2\mu\sin\theta\cos\Psi} = \frac{\sin^2\theta - \sin^2(\omega-\theta)}{2\mu\sin\theta\cos(\omega-\theta)} \tag{E.6}$$

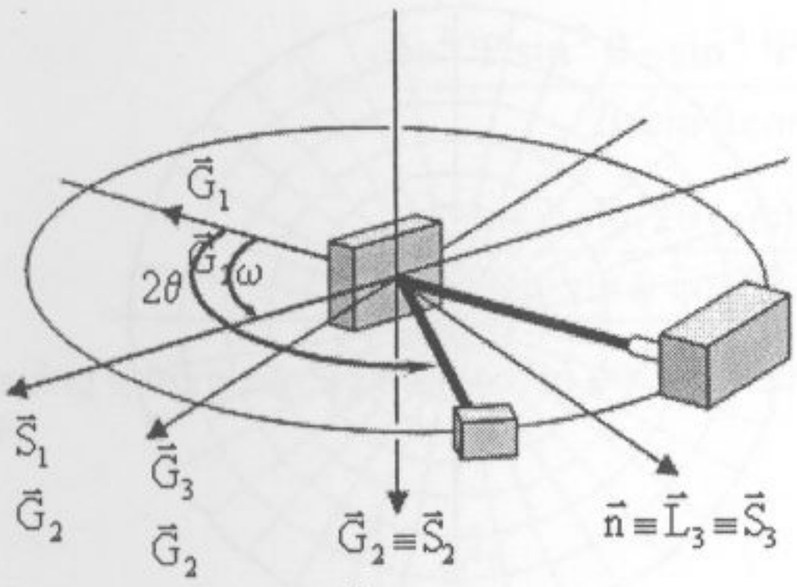

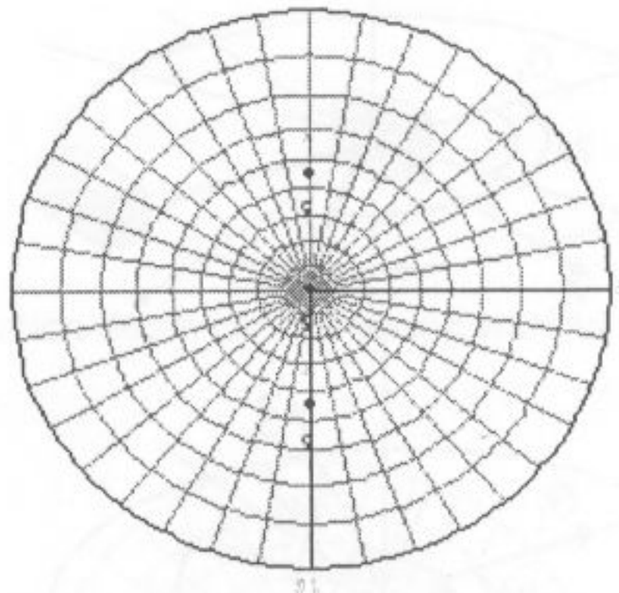

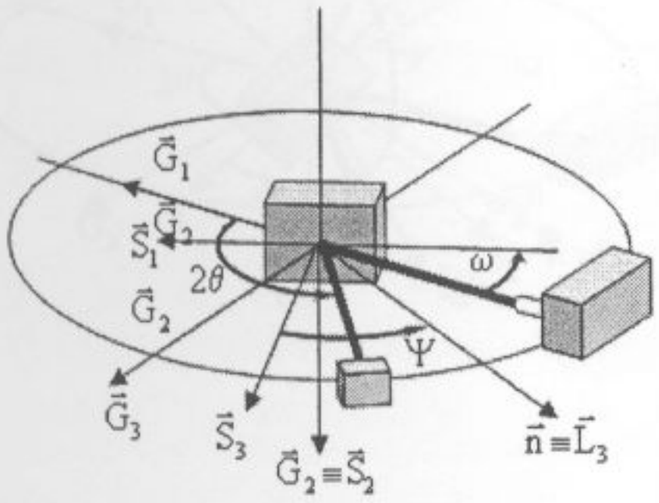

Key

$\left(\vec{S}_1, \vec{S}_2, \vec{S}_3\right)$ and $\left(\vec{G}_1, \vec{G}_2, \vec{G}_3\right)$ superposed reference systems

L_3 is normal to the diffracting {hkl} lattice planes

2θ The diffraction angle, this is the angle between the incident and diffracted X-ray beams

ω The angle between the incident X-ray beam and the specimen surface at $\chi = 0$

ψ The angle between the normal of the specimen and the normal of the diffracting planes

X The incident beam direction

° (open circle) The diffracted beam

• (black dot) The bisector of the incident and diffracted beams

Figure E.3 : Perspective drawing of the omega method for Φ=0 and Ψ=0 or Ψ=–45° (left). Stereographic representation for Φ=0 and three values of Ψ : -45°, 0, +45° (right).

E.3.3 Chi (χ) method

This mode is obtained by using the χ rotation of a Eulerian cradle to achieve the Ψ tilt and a 0D or 1D detector. In this case $\gamma = 0$, $\omega = \theta$ and $\eta = 0$. From formulae (E.1) to (E.4), it gives :

$$\begin{cases} \Psi = \chi \\ \Phi = \varphi + \pi/2 \end{cases} \tag{E.7}$$

with a penetration depth :

$$z = \frac{\sin\theta\cos\Psi}{2\mu} = \frac{\sin\theta\cos\chi}{2\mu} \tag{E.8}$$

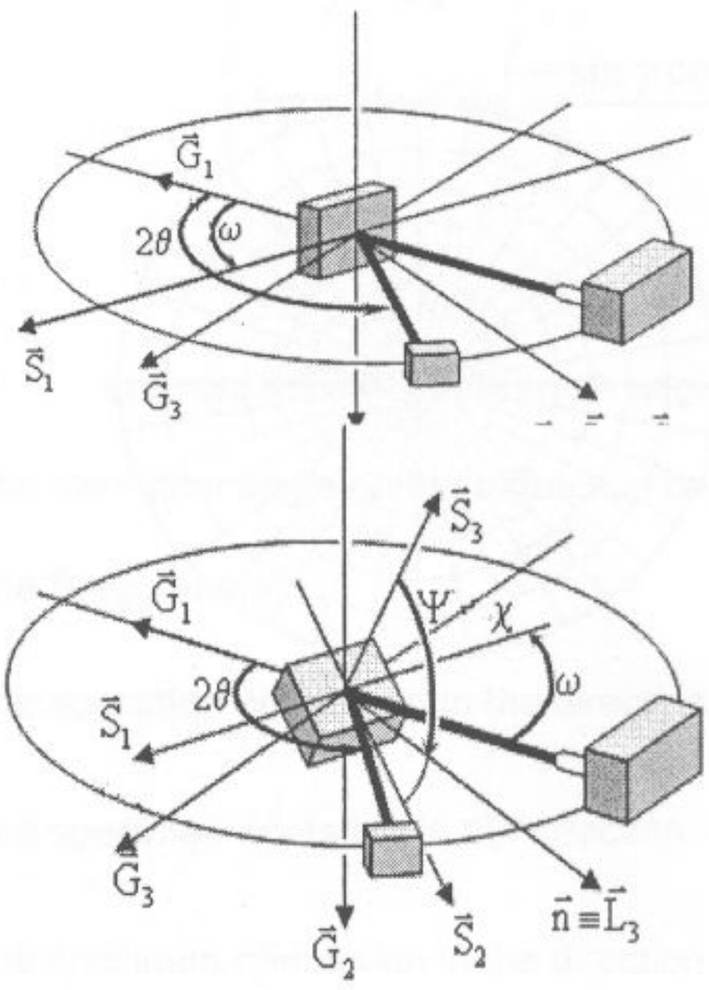

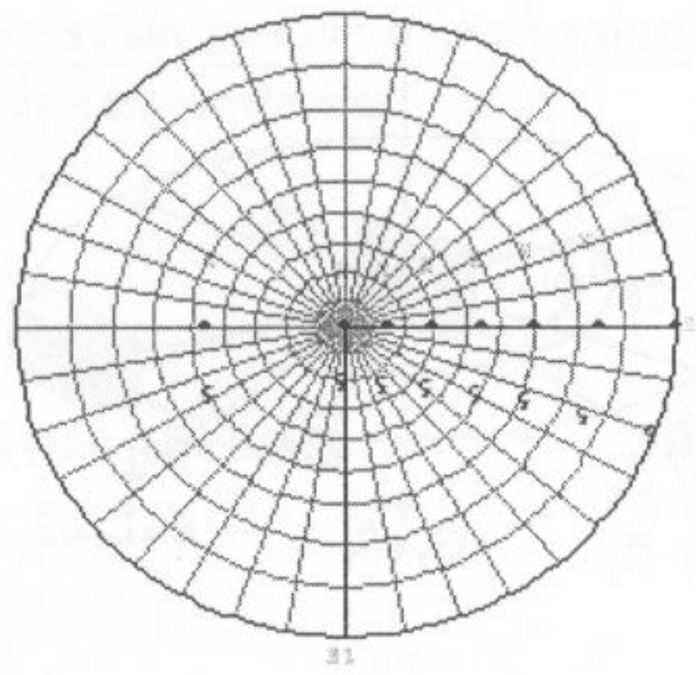

Key

$\left(\vec{S}_1, \vec{S}_2, \vec{S}_3\right)$ and $\left(\vec{G}_1, \vec{G}_2, \vec{G}_3\right)$ superposed reference systems

L_3 is normal to the diffracting {hkl} lattice planes

2θ The diffraction angle, this is the angle between the incident and diffracted X-ray beams

ω The angle between the incident X-ray beam and the specimen surface at $\chi = 0$

ψ The angle between the normal of the specimen and the normal of the diffracting planes

χ The angle χ rotates in the plane perpendicular to that containing ω and 2θ.

X The incident beam direction

° (open circle) The diffracted beam

• (black dot) The bisector of the incident and diffracted beams

Figure E.4 - Perspective drawing of the chi method for Φ=90° and Ψ=0 or Ψ=+60° (left). Stereographic representation for Φ=90° and 8 values of Ψ : –45°, 0, 15°, 30°, 45°, 60°, 75° et 90°. (right).

E.3.4 Combined tilt method (also called scattering vector method)

These are general acquisition modes that give penetration depths and optical aberrations that are in between the omega and chi modes. From arbitrary values of χ, φ and ω, the expressions of Ψ and Φ are given from formulae (E.1) and (E.2) :

$$\begin{cases} \Psi = \text{sign}(\omega-\theta)\,\text{ArcCos}\left(\cos\chi\cos(\omega-\theta)\right) \\ \Phi = \varphi + \Delta\varphi \quad \text{with} \quad \Delta\varphi = \text{ArcTan}\left(\dfrac{\sin\chi}{\tan(\omega-\theta)}\right) \end{cases} \tag{E.9}$$

For given values of Φ and Ψ there is an infinite set of (χ, φ, ω) values which can be obtained by rotating the incident and diffracted beams around the measurement direction $\vec{n}$ by an angle η. The penetration depth is given from formulae (E.3) and (E.4) with γ=0 :

$$z = \frac{\cos^2\Psi\sin^2\theta - \sin^2\Psi\cos^2\theta\sin^2\eta}{2\mu\sin\theta\cos\theta} \tag{E.10}$$

$$z = \frac{\cos\chi\,\sin(2\theta-\omega)\,\sin\omega}{2\mu\,\sin\theta\,\cos(\theta-\omega)} \tag{E.11}$$

By varying η from zero (χ method) to 90° (ω method), the penetration depth can be varied without changing Φ and Ψ.

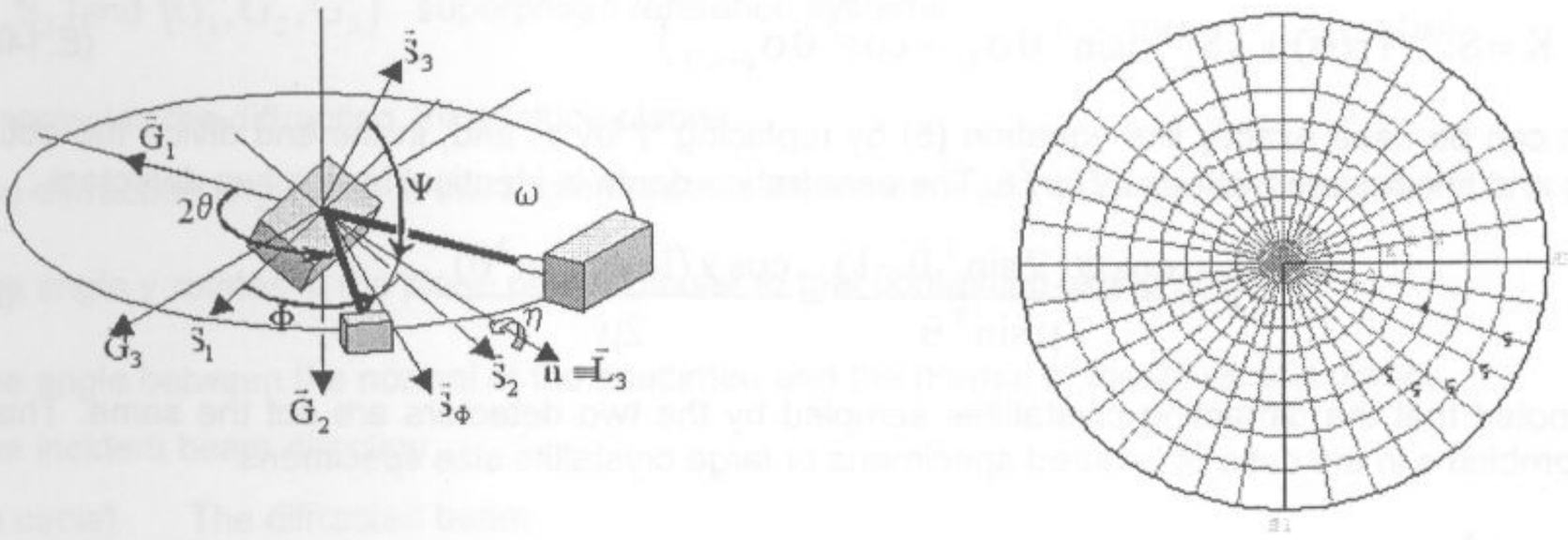

Key

$\left(\vec{S}_1, \vec{S}_2, \vec{S}_3\right)$ and $\left(\vec{G}_1, \vec{G}_2, \vec{G}_3\right)$ superposed reference systems

L_3 is normal to the diffracting {hkl} lattice planes

2θ The diffraction angle, this is the angle between the incident and diffracted X-ray beams

ω The angle between the incident X-ray beam and the specimen surface at χ =0

ψ The angle between the normal of the specimen and the normal of the diffracting planes

χ The angle χ rotates in the plane perpendicular to that containing ω and 2θ.

X The incident beam direction

° (open circle) The diffracted beam

• (black dot) The bisector of the incident and diffracted beams

Figure E.5 - Perspective drawing of the combined method for Φ = 70°, Ψ = 60° and η = 22.5° (left). Stereographic representation for Φ = 70°, Ψ = 60° and 5 values of η : 0, 22.5°, 45°, 67.5° and 90°..

E.3.5 Modified chi method

This mode is used on some portable goniometers with two detectors placed symmetrically on each side of the incident beam. Angle ω is set equal to $\pi/2$ so that at $\chi = 0$ the incident beam is normal to the specimen surface. The χ and φ rotations are used to vary the measurement direction. The use of two detectors allows to compensate for the $\Delta\varphi$ so that $\Psi \approx \chi$ with minor systematic errors on the $\sin^2\Psi$ slope (which can be easily corrected). For detector 1, angle γ is equal to zero and for detector 2, angle γ is equal to π.

$$\text{Detector 1}: \begin{cases} \Psi = \text{ArcCos}(\cos\chi \sin\theta) \\ \Phi = \varphi + \dfrac{\pi}{2} + \Delta\varphi \quad \text{with} \quad \Delta\varphi = \text{ArcTan}\left(\dfrac{-1}{\sin\chi \tan\theta}\right) \end{cases} \tag{E.12}$$

$$\text{Detector 2}: \begin{cases} \Psi = \text{ArcCos}(\cos\chi \sin\theta) \\ \Phi = \varphi + \dfrac{\pi}{2} + \Delta\varphi \quad \text{with} \quad \Delta\varphi = \text{ArcTan}\left(\dfrac{1}{\sin\chi \tan\theta}\right) \end{cases} \tag{E.13}$$

As can be seen, the two $\Delta\varphi$ compensate each other. Thus, when the strains measured by the two detectors are averaged they disappear. The measured strain (equation (5) of main text) can thus be written :

$$\varepsilon_{\phi\psi} = \tfrac{1}{2} S_2^{\{hkl\}} \sin^2\theta \sin^2\chi \left(\sigma_\phi - \sigma_{33}\right) + \tfrac{1}{2} S_2^{\{hkl\}} \sin^2\theta \sin 2\chi \, \tau_\phi + K \tag{E.14}$$

Where:

$$K = S_1^{\{hkl\}} \text{Tr}(\sigma) + \tfrac{1}{2} S_2^{\{hkl\}} \left(\sin^2\theta \, \sigma_{33} + \cos^2\theta \, \sigma_{\phi+\pi/2}\right) \tag{E.14bis}$$

This equation can be used exactly like equation (5) by replacing Ψ by χ, and, in the end divide the obtained normal stress and shear stress values by $\sin^2\theta$. The penetration depth is identical for the two detectors :

$$z = \frac{\cos\psi(2\sin^2\theta - 1)}{2\mu\sin^3\theta} = \frac{\cos\chi(1 - \text{cotan}^2\theta)}{2\mu} \tag{E.15}$$

It should be noted that the diffracting crystallites sampled by the two detectors are not the same. This can cause some problems in the case of textured specimens or large crystallite size specimens.

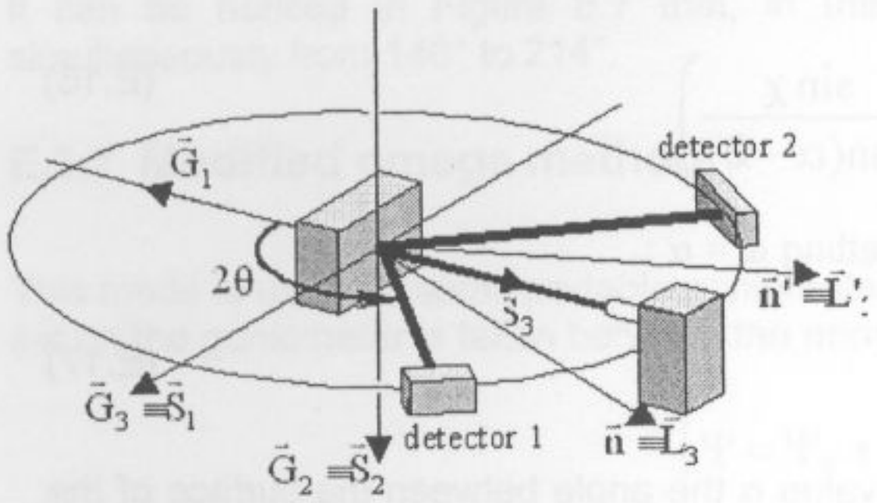

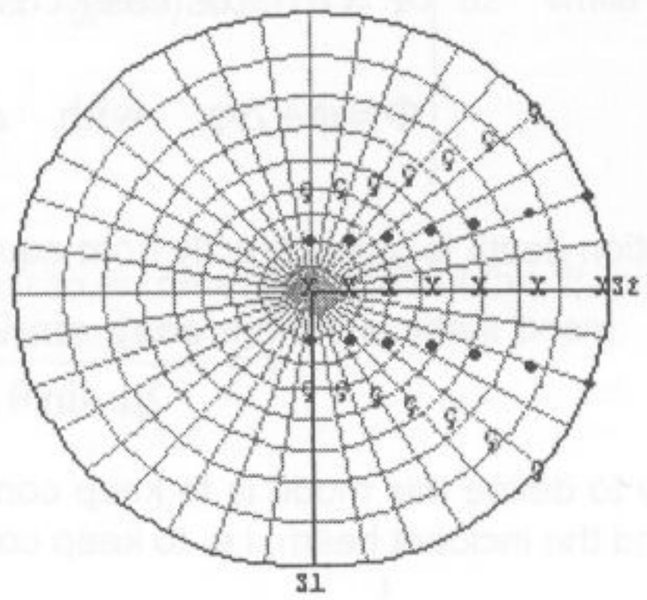

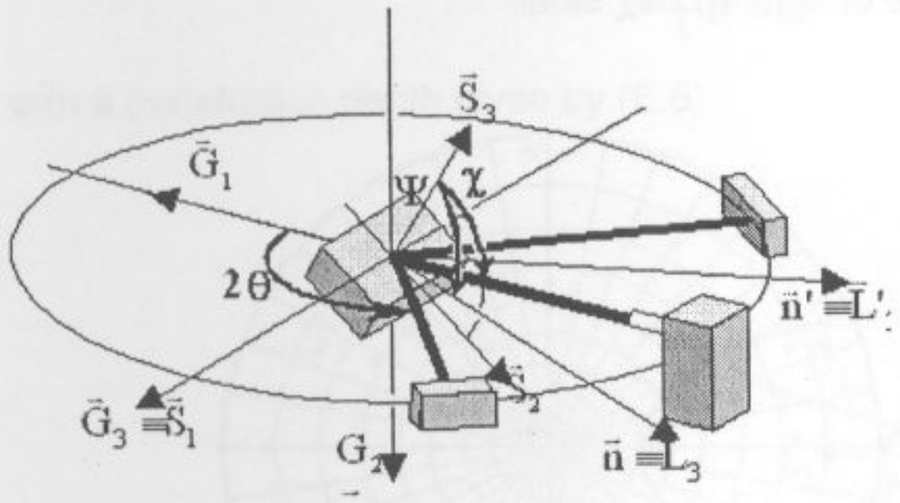

Key

$(\vec{S}_1, \vec{S}_2, \vec{S}_3)$ and $(\vec{G}_1, \vec{G}_2, \vec{G}_3)$ superposed reference systems

L_3 is normal to the diffracting {hkl} lattice planes

2θ The diffraction angle, this is the angle between the incident and diffracted X-ray beams

χ The angle χ rotates in the plane perpendicular to that containing ω and 2θ.

Ψ The angle between the normal of the specimen and the normal of the diffracting planes.

X The incident beam direction

° (open circle) The diffracted beam

• (black dot) The bisector of the incident and diffracted beams

Figure E.6 - Perspective drawing of the modified chi method (left). Starting position (up) with ω = 90°, φ = χ = 0. Position for χ = 60° et φ = 0 (down), which corresponds to a measurement in direction $\vec{S}_2$ i.e., after averaging the strains obtained from the two detectors, to the direction Φ = 90°. Stereographic representation for 2θ = 140°, ω = 90°, φ = 0 and 7 values of χ : 0, 15°, 30°, 45°, 60°, 75° and 90° (right).

It can be noticed in Figure E.6 that the values of Ψ are always greater than the corresponding values of χ. For detector 1, Ψ varies from 20° to 90° while Φ varies from 0 to 50°. Fir detector, Ψ varies from 20° to 90° while Φ varies from 180° to 130°.

E.3.6 Low incidence method

This mode is used to achieve shallow penetration depth and wide irradiated surfaces. The idea is to set ω at a fixed value α typically 2 to 5°. The χ and φ rotations are used to vary the measurement direction. A 0D detector with long Soller slits is used to reduce optical aberrations so γ = 0 :

$$\begin{cases} \Psi = \mathrm{ArcCos}\left(\cos\chi\cos(\alpha-\theta)\right) \\ \Phi = \varphi + \Delta\varphi \quad \text{with} \quad \Delta\varphi = \mathrm{ArcTan}\left(\dfrac{\sin\chi}{\tan(\alpha-\theta)}\right) \end{cases} \tag{E.16}$$

The penetration depth is given directly from equation (E.11) by setting $\omega = \alpha$:

$$z = \frac{\cos\chi\ \sin(2\theta-\alpha)\ \sin\alpha}{2\mu\ \sin\theta\ \cos(\theta-\alpha)} \tag{E.17}$$

Another way to define this mode is to keep constant at a given value α the angle between the surface of the specimen and the incident beam, i.e. to keep constant the value of $\sin\alpha = \cos\chi\ \sin\omega$.

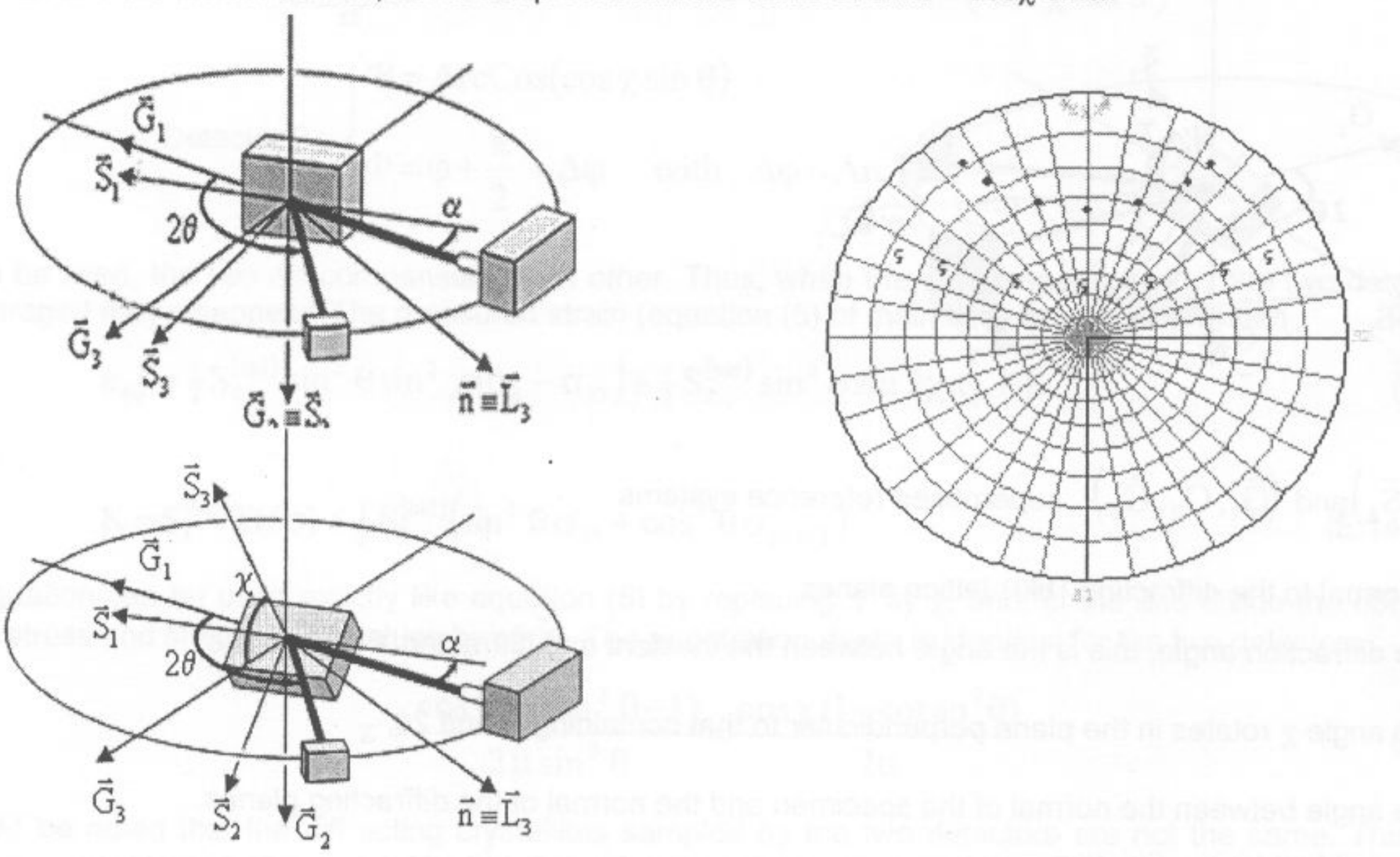

Key

$\left(\vec{S}_1, \vec{S}_2, \vec{S}_3\right)$ and $\left(\vec{G}_1, \vec{G}_2, \vec{G}_3\right)$ superposed reference systems

L_3 is normal to the diffracting {hkl} lattice planes

2θ The diffraction angle, this is the angle between the incident and diffracted X-ray beams

χ The angle χ rotates in the plane perpendicular to that containing ω and 2θ.

α is a fixed value of ω tipically comprised beteen 2 and 5 degrees

X The incident beam direction

° (open circle) The diffracted beam

• (black dot) The bisector of the incident and diffracted beams

Figure E.7 - Perspective representation of the low incidence mode (left). On top, starting position with $\omega = \alpha$, $\chi = \varphi = 0$. Down, position for $\chi = 60°$ and $\varphi = 0$. Stereographic representation for $\omega = \alpha = 5°$, $2\theta = 120°$, $\varphi = 0$ and 7 values of χ : -75°, -60°, -30°, 0, 30°, 60°, 75°.

It can be noticed in Figure E.7 that, in this configuration, Ψ varies from 55° to 82° while Φ varies simultaneously from 146° to 214°.

E.3.7 Modified omega method

This mode is used on some portable goniometers. It is very similar to an omega mode but the Ψ_0 angle that is set on the goniometer is taken between the normal to the specimen surface and the incident beam.

$$\begin{cases} \Psi = \Psi_0 + \dfrac{\pi}{2} - \theta \\ \Phi = \varphi \end{cases} \tag{E.18}$$

with a penetration depth given by (E.6).

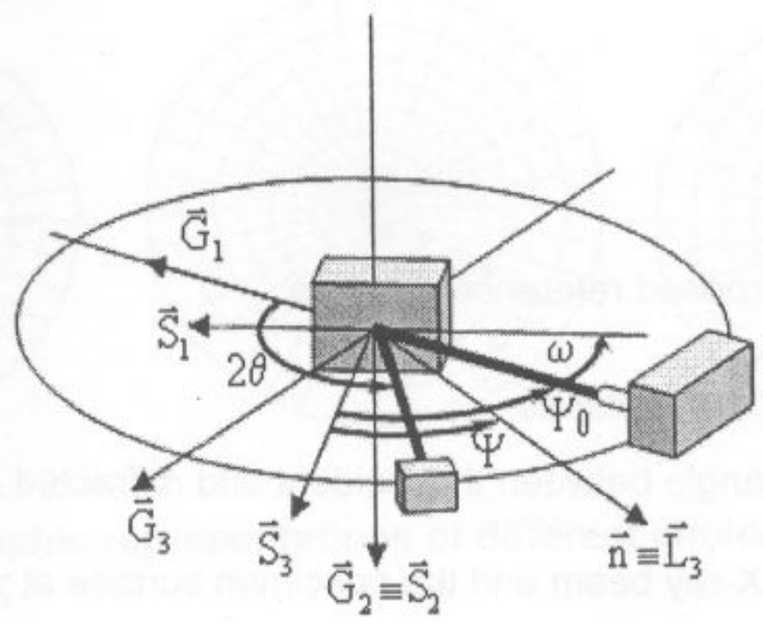

Key

(S_1, S_2, S_3) Specimen coordinate system.

$\left(\vec{G}_1, \vec{G}_2, \vec{G}_3\right)$ Goniometer reference system

(L_1, L_2, L_3) Laboratory coordinate system.

2θ The diffraction angle, this is the angle between the incident and diffracted X-ray beams

Figure E.8 - Perspective drawing of the modified omega method.

By comparing with figure E.3, it is clear that the two methods only differ through the origin in Ψ.

E.3.8 Use of a 2D (area) detector

The use of a 2D detector allows to acquire a whole section of the diffraction cone (of the Debye ring), i.e. a whole range of γ values. According to equations (E.1) and (E.2), it corresponds to a whole range of Ψ and Φ values. Theoretically, one acquisition is sufficient to obtain enough information for calculating some stress components, however, in practice, the acquisition range in Ψ is too small to give reasonable accuracies. At least a second acquisition for another value of χ, ω or φ is advised. The relevant equations for this method are (E.1) to (E.4), i.e. the general equations.

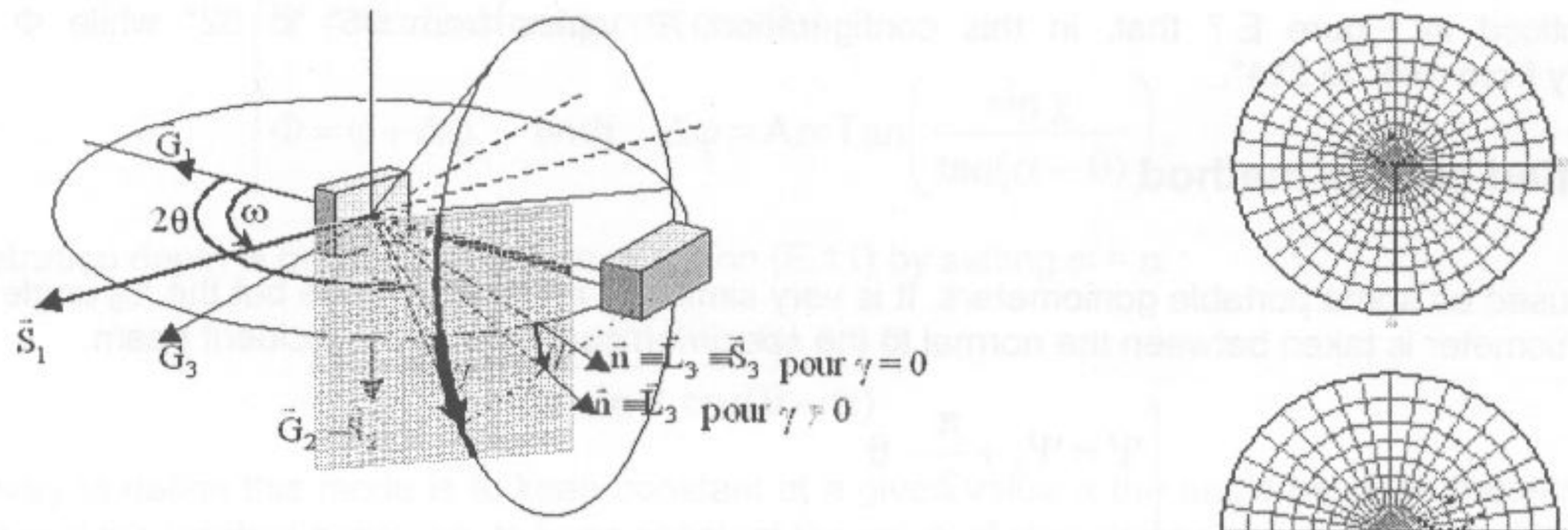

Key

$\left(\vec{S}_1, \vec{S}_2, \vec{S}_3\right)$and $\left(\vec{G}_1, \vec{G}_2, \vec{G}_3\right)$ superposed reference systems

L_3 is normal to the diffracting {hkl} lattice planes

2θ The diffraction angle, this is the angle between the incident and diffracted X-ray beams

ω The angle between the incident X-ray beam and the specimen surface at χ =0

X The incident beam direction

° (open circle) The diffracted beam

• (black dot) The bisector of the incident and diffracted beams

Figure E.9 -Perspective representation of a possible set-up to work with a 2D detector for ω = θ = 70° and χ = φ = 0 (left).

In Figure E.9 a plane detector is shown, but cylindrical detectors also exist. The detector acquires a section of the diffraction cone for γ varying from -45° to +45°. On the right, stereographic representation for ω = θ = 70° and φ = 0 and 9 values of γ: -60°, -45°, -30°, -15°, 0, 15°, 30°, 45°, 60°. On top, representation for χ = 0 : it can be seen that Ψ varies from 0 to 20° while Φ varies simultaneously from -90° to +90°. Down, representation for χ = 40°, Ψ varies from 22° to 58° while Φ varies from 90° to *115°*.

E.4 Choice of Φ and Ψ angles

When measurements are performed in only one direction Φ, the minimum number of tilt angle Ψ is 2 for a biaxial stress state and 3 for a triaxial stress state. However, due to sampling effects linked to the microstructure of the material, it is generally acknowledged that this minimum is actually not sufficient. That is why the present standard recommends 4 or 5 tilts for the biaxial case and 7 for the triaxial case.

The same question arises for tensor analysis. The minimum number of (Φ, Ψ) couples is 6, taken in, at least, 3 independent Φ directions. Several ways are possible to choose the Φ directions. One of the most common is to take :

$$\Phi = 0,\ 45° \text{ and } 90° \text{ with positive and negative } \Psi \text{ values} \qquad \text{(E.19)}$$

However, as it can be seen on a stereographic representation, this is not the best sampling possible, i.e., the directions are not spread as uniformly as possible in the whole available solid angle. If three Φ directions are

chosen, a better choice is :

Φ = 0, 60° and 120° with positive and negative Ψ values (E.20)

Whether (E.19) or (E.20) is chosen is the same problem as for rosette strain gauges : if the principal stresses are known before the measurement, (E.19) is easier to use, but if they are not known, (E.20) will be more accurate.

More than three directions can be chosen. It is necessary to check the consistency of the results, to calculate the uncertainty on the stress components and it will increase the overall accuracy of the measurement. It is thus advised to use at least four Φ directions. If n is the number of directions, the Φ values can be separated by :

$$\Delta\Phi = 180°/n \quad \text{(E.21)}$$

For instance, for five Φ directions, the Φ values can be : 0, 36°, 72°, 108° and 144°.

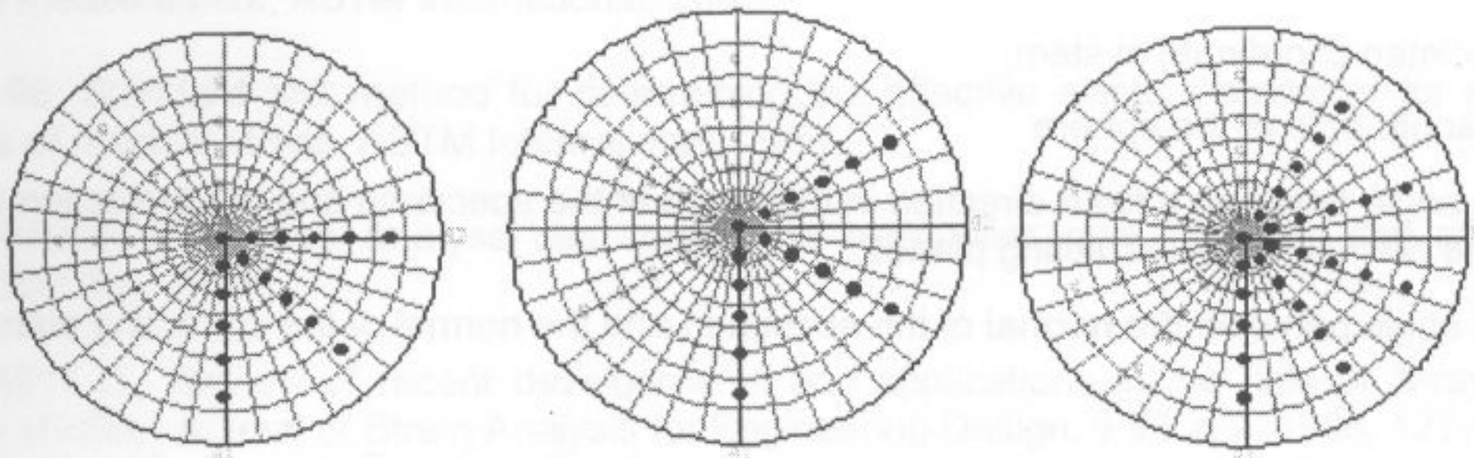

Figure E.10 : stereographic representations of different choices for the Φ directions.

In Figure E.10 on the left, three directions are chosen according to (E.19). On the middle, three directions are chosen according to (E.20) or (E.21). On the right, five directions are chosen according to (E.21).

E.5 The stereographic projection

The stereographic projection is a useful tool to represent accurately directions (crystallographic directions, measurement directions, diffracted and incident beams...) emanating from a specimen which is assumed punctual and located at the origin O of the reference system $(\vec{S}_1, \vec{S}_2, \vec{S}_3)$. The direction of interest intersects a sphere of radius R centred on O. The intersection point is then projected on to the $(\vec{S}_1, \vec{S}_2)$ plane of the specimen surface. The projection issues from a centre H which is the south pole of the sphere.

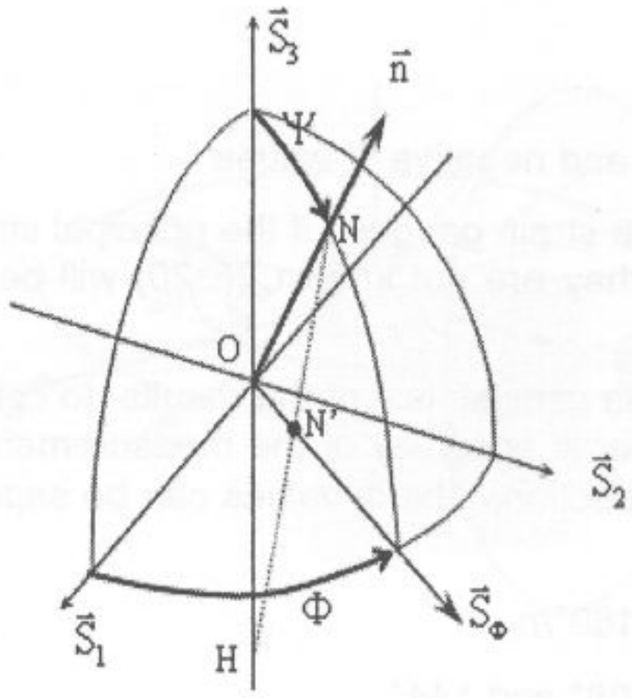

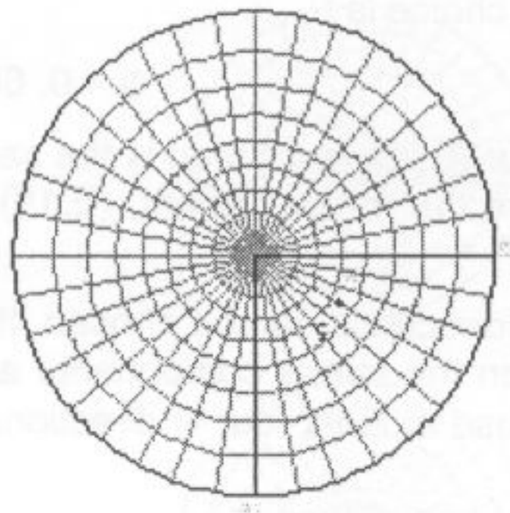

Key

S_1, S_2, S_3	Specimen coordinate system.
H	the south pole of the sphere
Φ	The angle between a fixed direction in the plane of the specimen and the projection in that plane of the normal to the diffracting planes.
Ψ	The angle between the normal of the specimen and the normal of the diffracting planes.

Figure E.11 - Example of a stereographic representation of a direction $\vec{n}$ described by angles $\Phi = 60°$ and $\Psi=45°$ (right).

In Figure E.11 the angle Φ can be read directly on the projection and angle Ψ can be read along a radius of the projection circle. On the perspective drawing on the left, only one eighth of the sphere is represented.

For instance, let's take a direction $\vec{n}$ described by the two angles Φ and Ψ. The straight line directed by $\vec{n}$ intersects the sphere at point N. The line (HN) intersects the plane $(\vec{S}_1,\vec{S}_2)$ at point N' which is the stereographic projection of $\vec{n}$ (black dot on figure E.10). The coordinates of N' in the reference system $(\vec{S}_1,\vec{S}_2)$ are :

$$\begin{cases} x = R\cos\Phi\tan\left(\frac{\Psi}{2}\right) \\ y = R\sin\Phi\tan\left(\frac{\Psi}{2}\right) \end{cases}$$

To make the use of a stereographic projection easier, it is graduated every 10° in Φ and every 10° in Ψ. The $\vec{S}_3$ direction (corresponding to Ψ=0) is at the centre of the projection circle while the direction for which Ψ=90° are located on the external edge of the circle. Thus, on figure E.10, the values of Φ (60°) and Ψ (45°) can be read directly and unambiguously. The incident beam (X mark) and the diffracted beam (white dot) can also be represented clearly as compared with a perspective drawing that would be confusing.

Bibliography

HAUK V., BEHNKEN H., REIMERS W., PFEIFFER W., GENZEL Ch. et al. Structural and Residual Stress Analysis by Non-destructive Methods, Elsevier, 1997, ISBN 0 444 824 766

NOYAN I.C. and COHEN J.B., Residual Stress: Measurement by Diffraction and Interpretation, Springer-Verlag, 1987

Handbook of Residual Stress and Deformation in Steel, ASM International, 2002

ASTM E915-96, Standard test method for verifying the alignment of x-ray diffraction instrumentation for residual stress measurement, ASTM International, 2002

ASTM E1426-98, Standard test method for determining the effective elastic parameter for x-ray diffraction measurements of residual stress, ASTM International, 2003

LODINI A., PERRIN M. editors Analyse des contraintes résiduelles par diffraction des rayons X et des neutrons, INSTN/CEA, 1996.

LU J., RETRAINT D., Review of recent developments and applications in the field of X-ray diffraction for residual stress studies, Journal of Strain Analysis for Engineering Design, v 33, n 2, 1998, 127-136

FITZPATRICK M.E., FRY A.T., HOLDWAY P., KANDIL F.A., SHACKLETON J. and SUOMINEN L.: NPL Good Practice Guide No. 52: Determination of Residual Stresses by X-ray Diffraction. March 2002 ISSN 1368-6550

SCHOLTES, B., Verfahrensbeschreibung - Röntgenographische Ermittlung von Spannungen - Ermittlung und Bewertung homogener Spannungszustände in kristallinen, makroskopisch isotropen Werkstoffen. Arbeitsgemeinschaft Wärmebehandlung und Werkstofftechik e.V. (AWT), 2000.

---

1. prEN ISO TS 21432 "Non-destructive testing - Test method for measurement of residual stress by neutron diffraction"

2. MOORE M.G., EVANS W.P., Mathematical correction for stress in removed layers in X-ray diffraction residual stress analysis, SAE Transactions, vol 66, 1958, 340-345; Handbook on Techniques of Residual Stresses Measurement", SEM (American Society for Experimental Mechanics), J. Lu and M.R. James editors, 1996).

3. E1237-93(2003) "Standard Guide for Installing Bonded Resistance Strain Gages" ASTM International

4. PFEIFFER W.: A new intensity and background correction procedure for Ω-diffractometers. Materialprüfung 37, 7-8, s292-295(1995)

5. FRANÇOIS M. et al. Reference specimens for x-ray stress analysis: the French experience, Metrologia 41 (2004) 33-40

6. FRANÇOIS M., LEBRUN J.L., X-ray stress determination on materials with large size crystallites-theoretical approach, Proc. of the 3rd European Conf. on Residual Stresses (ECRS 3), 4-6 nov. 1992, Frankfurt, Germany.

7. HENNION V., SPRAUEL J.M. and MICHAUD. H. "Contribution to residual–stress evaluation in high-stress-gradient zones by X-ray diffraction" J.Appl.Cryst. (2000). **33**, 26-34

8. FRANÇOIS M., DIONNET B., SPRAUEL J.M., NARDOU F., The influence of cylindrical geometry on X-ray stress tensor analysis, part I, general formulation, J. of Applied Crystallography, vol.28, 1995, 761-767.

9. DIONNET B., FRANÇOIS M., SPRAUEL J.M., NARDOU F., The influence of cylindrical geometry on X-ray stress tensor analysis, part II : applications, J. Appl. Cryst. (1999) 32, 883-891.

10. HAUK V., BEHNKEN H., REIMERS W., PFEIFFER W., GENZEL Ch. et al. Structural and Residual Stress Analysis by Nondestructive Methods, Elsevier, 1997, ISBN 0 444 824 766.

11. HE B. B., *The 20th ASM Heat Treating Society Conference Proceedings, Vol.1,* pp 408-417, St. Louis, Missouri, 2000.

12. GENZEL Ch., A Self-Consistent Method for X-Ray Diffraction Analysis of Multiaxial Residual Stress Fields in the Near Surface Region of Polycrystalline Materials. I. Theoretical Concept. J. Appl. Cryst., 32 (1999), 770 - 778.

13. GENZEL Ch., BRODA M., DANTZ D., REIMERS W., A Self-Consistent Method for X-Ray Diffraction Analysis of Multiaxial Residual Stress Fields in the Near Surface Region of Polycrystalline Materials. II. Examples. J. Appl. Cryst., 32 (1999), 779 - 787.

14. SPRAUEL J.M. and MICHAUD H. "Global X-ray method for determination of stress profiles" Materials Sciences forum Vols 404-407 (2002) pp 19-24

15. PFEIFFER W. (1994). The role of the peak location method in X-ray stress measurement. Proc. of the Fourth Int. Conf. on Resid. Stresses. SEM, Bethel, CT, USA, 148-155.